Supplementary Information for

Sex bias in social deficits, neural circuits and nutrient demand in *Cttnbp2* autism models

Tzu-Li Yen, Tzyy-Nan Huang, Ming-Hui Lin, Tsan-Ting Hsu, Ming-Hsuan Lu, Pu-Yun-Shih, Jacob Ellegood, Jason Lerch and Yi-Ping Hsueh*

* Correspondence and requests for materials should be addressed to Yi-Ping Hsueh (yph@gate.sinica.edu.tw)

The PDF file includes Supplementary figures and legends, Supplementary methods and Supplementary Tables:

Supplementary Table 2 List of brain regions subjected to C-FOS staining and the *P* values for the comparisons among four groups (related to Fig. 2).

Supplementary Table 3 Ratios of mean C-FOS+ cell density across 31 brain regions (related to Fig. 2A).

Supplementary Table 4 Differentially expressed proteins in ILA synaptic proteomes between male M120I mutant and male wild-type mice (related to Fig. 4).

Supplementary Table 5 Differentially expressed proteins in ILA synaptic proteomes between female M120I mutant and female wild-type mice (related to Fig. 4).

Supplementary Table 6 Disease association of female differentially expressed proteins in ILA synaptic proteomes (related to Fig. 4).

Supplementary Table 7 Statistical methods and results (related to Fig. 1, 3, 4, 5 and 6).

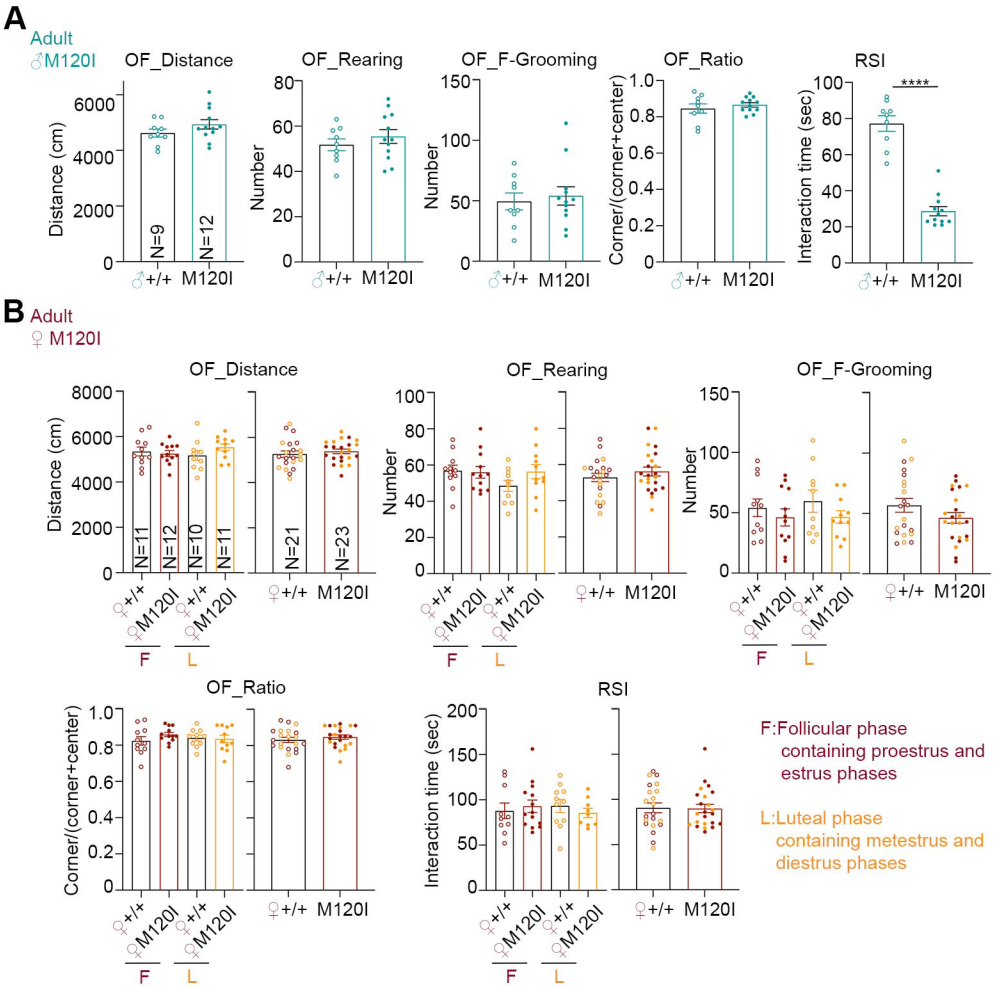

Supplementary Fig. 1. *Cttnbp2* M120I mutation impairs the social behaviors of male mice but not females in the adult stage (related to Fig. 1). (**A**) Adult male M120I mice of line #12 behave normally in an open field (OF), according to the total travel distance, rearing event number, grooming event number, and the ratio of the time spent in corners to the sum of time spent in the corners and the central area. However, M120I mutation does reduce the social behaviors of adult males in reciprocal social interaction (RSI). (**B**) In adult female mice, M120I mutation does not influence social behaviors or other behaviors in an open field, regardless of estrus cycle. Mouse estrus cycle has been separated into the follicular phase (proestrus and estrus phases) and the luteal phase (metestrus and diestrus phases). The sample sizes (*N*, i.e., numbers of mice) are indicated. Data are presented as means ± SEM, and the data points of individual mice are shown. ****, $P < 0.0001$. Two-tailed unpaired *t* test.

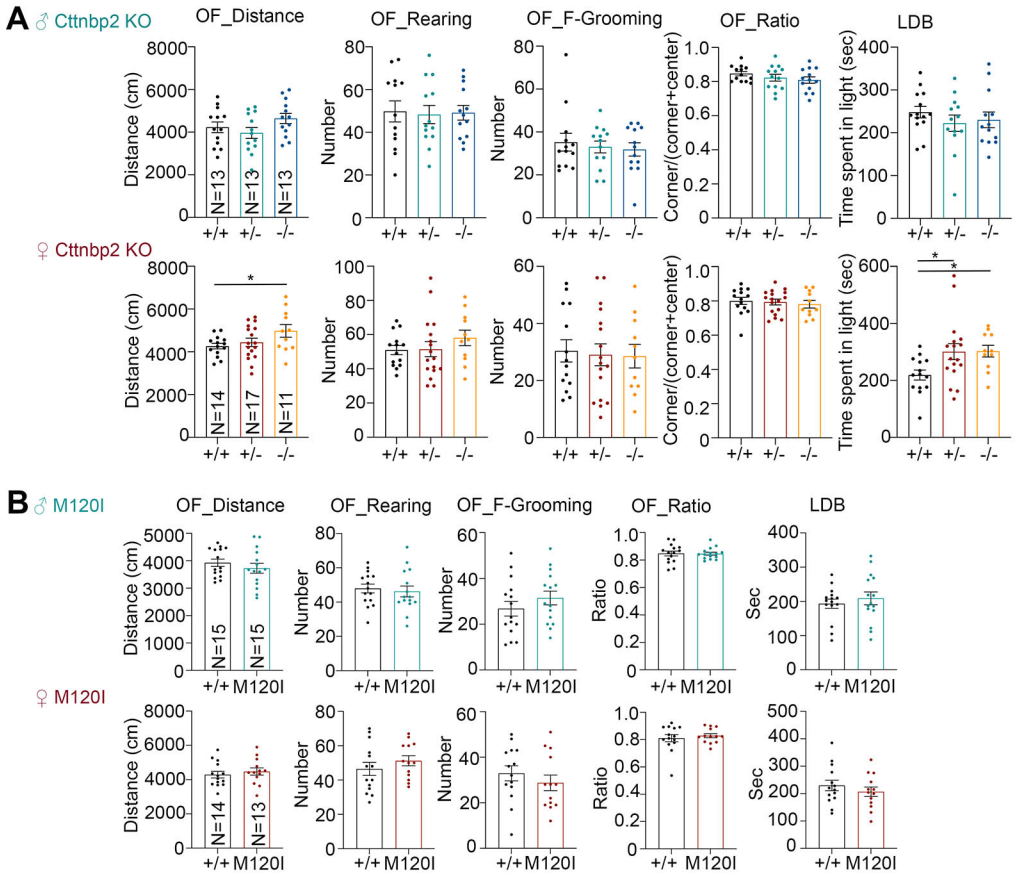

Supplementary Fig. 2. Behaviors of *Cttnbp2*$^{+/-}$, *Cttnbp2*$^{-/-}$ and M120I mice in an open field and light/dark box (related to Fig. 1). All experiments in this figure were conducted on juvenile mice younger than P42. (**A**) The behaviors of *Cttnbp2*$^{+/-}$ and *Cttnbp2*$^{-/-}$ mice in an open field (OF) and light-dark box (LDB). Upper: male; lower: female. Male mutant mice behaved normally in these two tests. Female mutant mice exhibited higher locomotor activity and anxiolytic behaviors. (**B**) The M120I mutant mice behave normally compared to their wild-type littermates, independently of sex. The sample sizes (*N*, i.e., numbers of mice) are indicated only in the left-most panels. Data are presented as means ± SEM, and the data points of individual mice are shown. * $P < 0.05$; **, $P < 0.01$. One-way ANOVA was used in (**A**). Two-tailed unpaired *t* test was used in (**B**).

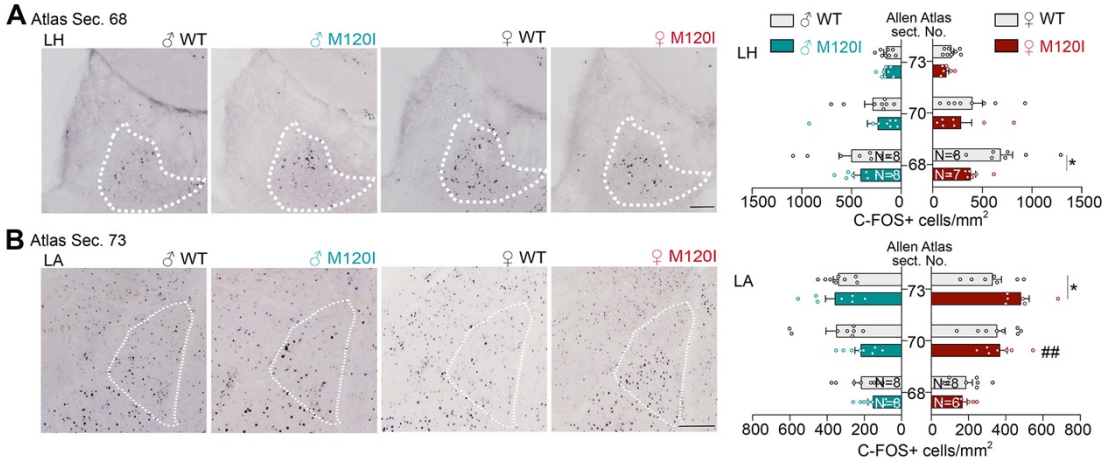

Supplementary Fig. 3. The brain regions of female M120I mice differentially respond to social stimulation (related to Fig. 2). Two hours after reciprocal social stimulations at P42 (**Fig. 1A**), C-FOS staining was performed to identify differentially activated brain regions of male and female *Cttnbp2* M120I mice. Only the lateral habenula (LH) and lateral amygdala (LA) were altered in female mutant mice, as shown in (**A**) and (**B**), respectively. Note that neuronal activity was reduced in the LH but increased in the LA of female mutant mice. The numbers (*N*) of mice examined are indicated. Data are presented as means ± SEM and individual data points are shown. *, $P < 0.05$, the comparison between female WT and M120I mice; ##, $P < 0.01$, the comparison between male and female mutant mice. Two-tailed unpaired *t* test. Scale bar: (**A**) 100 μm; (**B**) 250 μm.

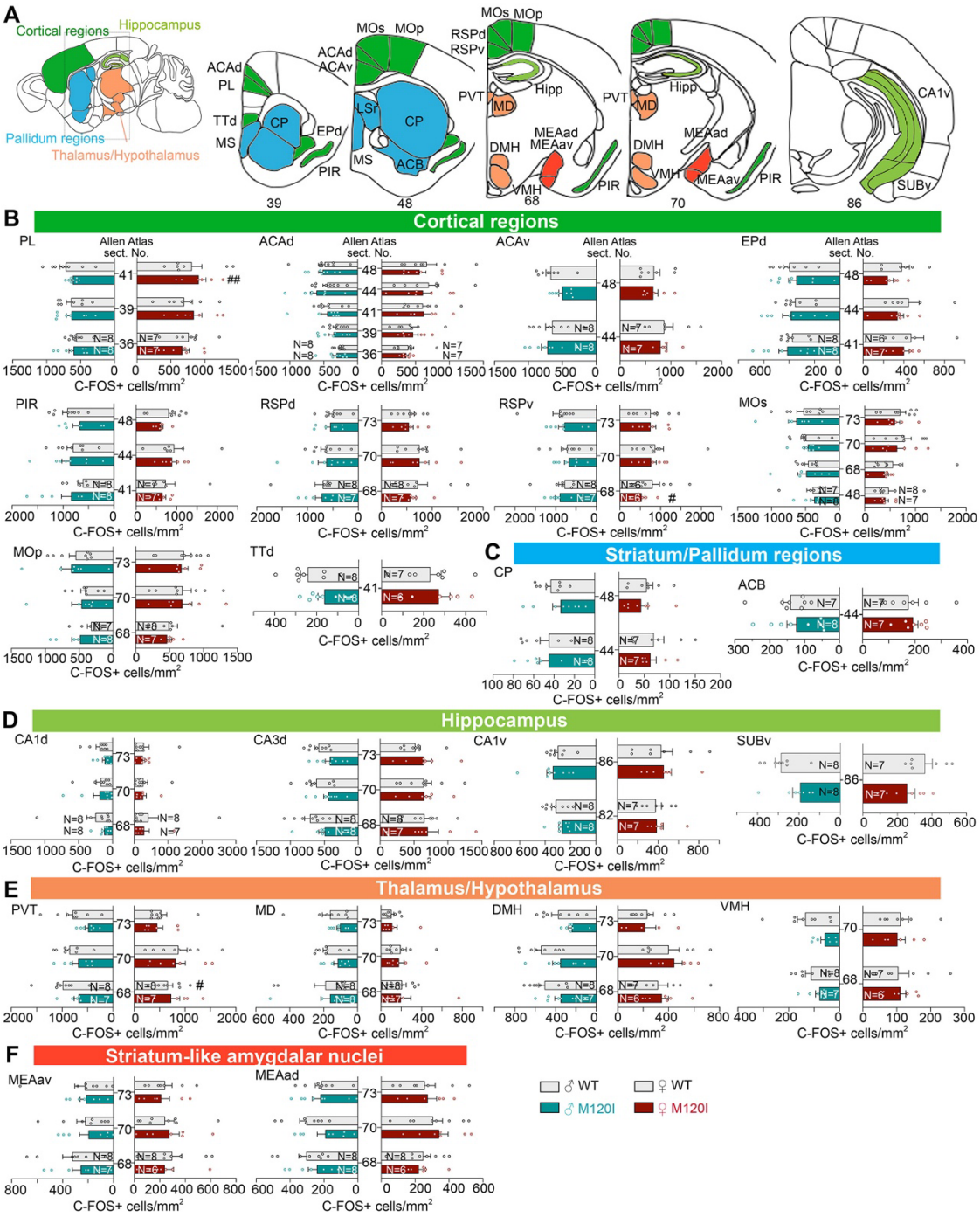

Supplementary Fig. 4. Brain regions do not show differential neuronal activation between genotypes upon social stimulation (related to Fig. 2). In addition to the brain regions shown in Figures 2 and S2, the results of C-FOS staining in the remaining brain regions assessed are summarized here. Full names of the brain regions are listed in **Supplementary Table 2**. (**A**) Schematic diagrams of brain sections. Different brain regions are highlighted with different colors. The corresponding section numbers based on the Allen Brain Atlas are indicated. (**B**)-(**F**) C-FOS-positive cell densities. Both male and female WT and *Cttnbp2* M120I mutant mice were analyzed. Each set of results presents data from male and female mice in the left and right panels, respectively. (**B**) Cortical region. (**C**) Striatum and pallidum regions. (**D**) Hippocampus. (**E**) Thalamus

and hypothalamus. (**F**) Striatum-like amygdalar nuclei. The numbers (*N*) of mice examined are indicated. In general, 6-8 mouse brains were used for each group. Data are presented as means ± SEM and individual data points are shown.. #, $P < 0.05$; ##, $P < 0.01$; comparison between male and female mice with the same genotype. Two-tailed unpaired *t* test.

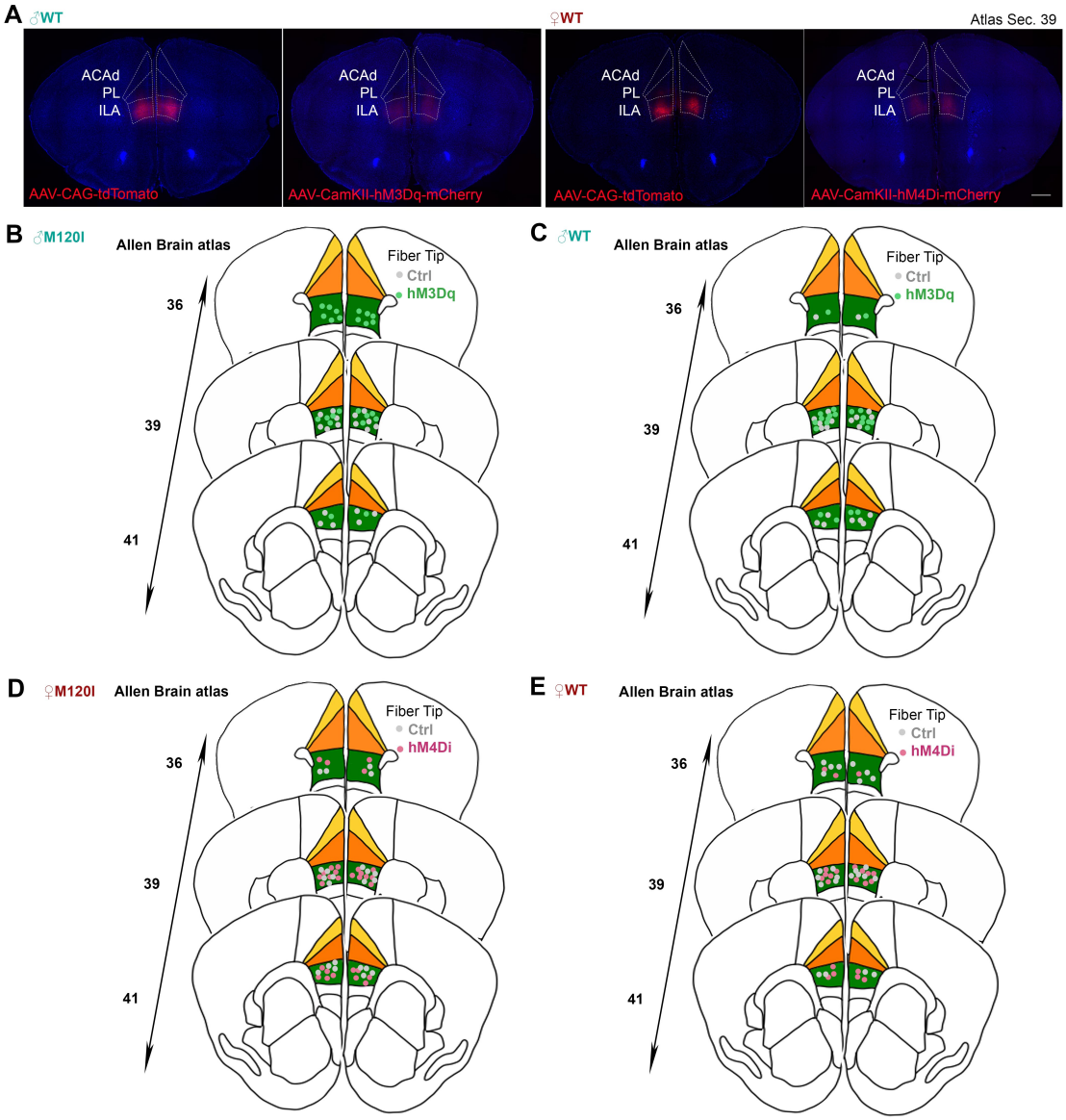

Supplementary Fig. 5. Summary of AAV expression and injection sites (related to Fig. 3). (**A**) Representative images of AAV expression at the injection site of the ILA. In addition to the ILA, the PL and ACAd regions are also indicated. Immunofluorescence signals of tdTomato and mCherry were used to monitor AAV expression. (**B**)-(**E**) AAV injection sites. (**B**) Male M120I mice were injected with AAV-CaMKII-hM3Dq-mCherry or AAV-CAG-tdTomato as a control (related to **Fig. 3C**). (**C**) Male WT mice injected with AAV-CaMKII-hM3Dq-mCherry or AAV-CAG-tdTomato as a control (related to **Fig. 3D**). (**D**) Female M120I mice injected with AAV-CaMKII-hM4Di-mCherry or AAV-CAG-tdTomato as a control (related to **Fig. 3E**). (**E**) Female WT mice injected with AAV-CaMKII-hM4Di-mCherry or AAV-CAG-tdTomato as a control (related to **Fig. 3F**). The Allen's Brain Atlas was used to identify brain regions, with corresponding section numbers indicated. Scale bar: 500 μm.

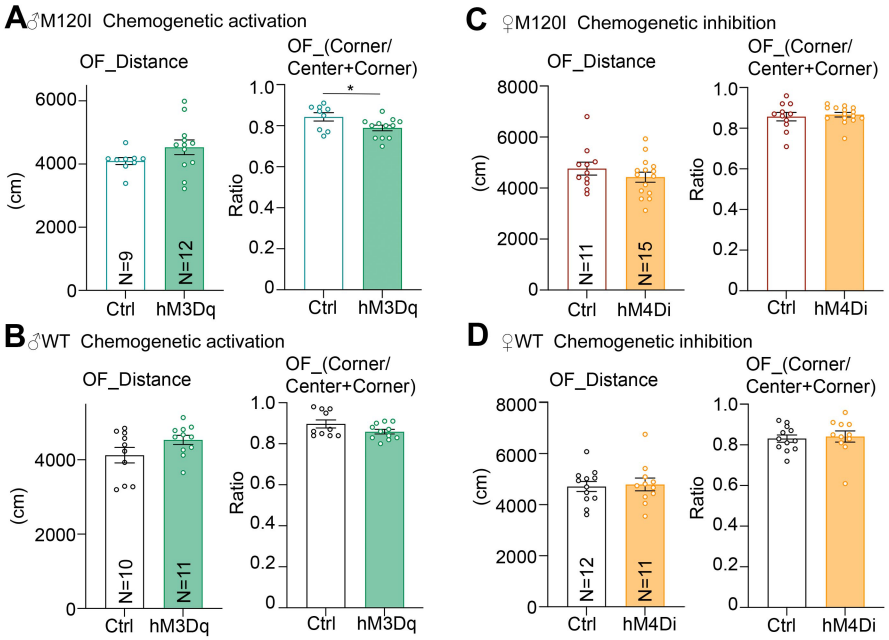

Supplementary Fig. 6. Chemogenetic manipulation does not alter mouse behaviors in an open field (related to Fig. 3). Before the social behavioral assays shown in **Figure 3**, all mice were analyzed in an open field test to determine the effect of surgery and expression of hM3Dq or hM4D1 on locomotor activity and anxiety. The results of open field are summarized here. The data of social interaction are shown in **Fig. 3C-3F**. Data are presented as means ± SEM and individual data points are shown. The numbers (*N*) of examined mice are indicated. *, $P < 0.05$; **, $P < 0.01$; ***, $P < 0.001$; ****, $P < 0.0001$. Two-tailed unpaired *t* tests.

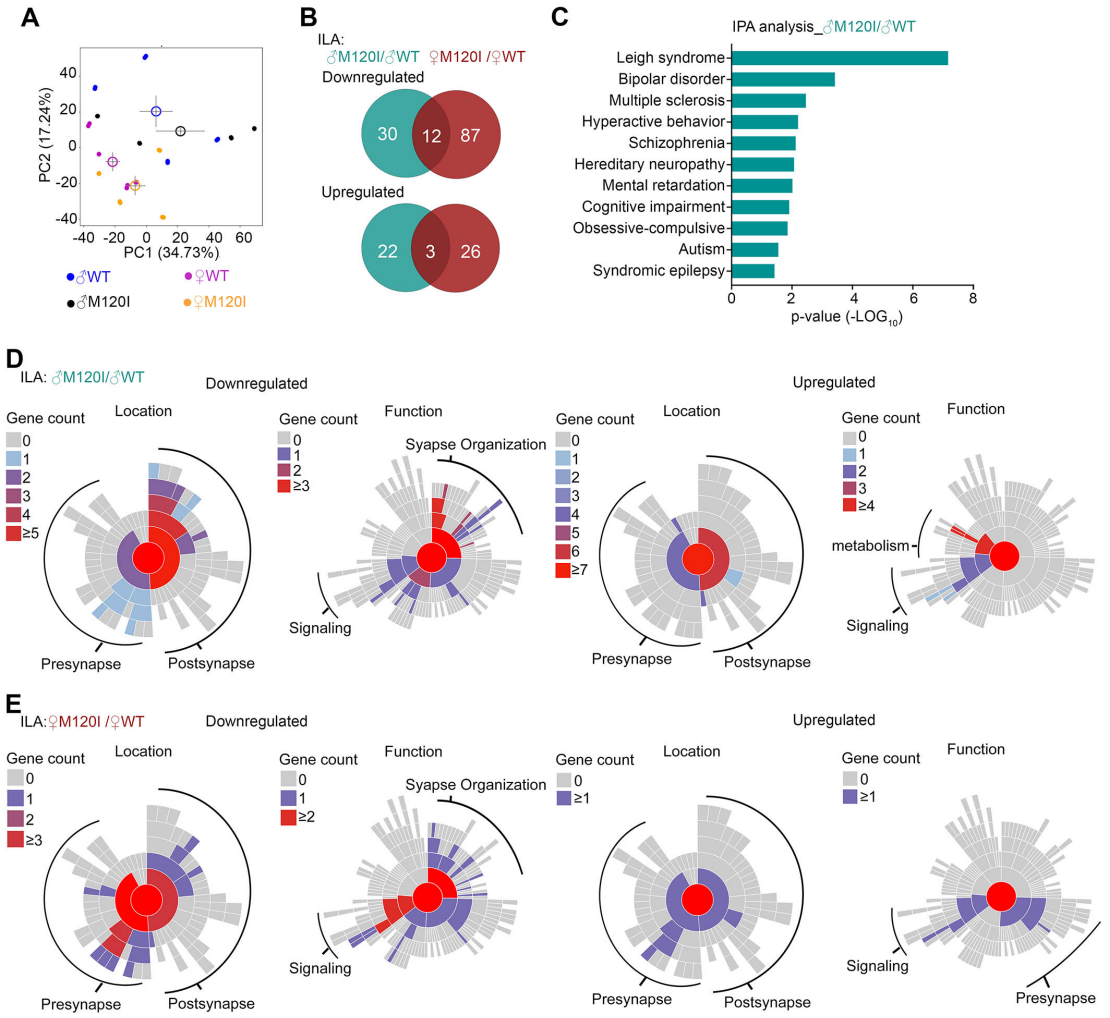

Supplementary Fig. 7. Bioinformatic analysis of synaptic proteomes (related to Fig. 4). (**A**) Principal component analysis of synaptic proteomes. Principal components 1 (PC1) and 2 (PC2) account for 34.73% and 17.24% of the data variability, respectively. (**B**) Venn diagram of differentially expressed proteins (DEPs) identified from the comparisons of ♂M120I vs. ♂WT and ♀M120I vs. ♀WT. The numbers of DEPs for each group are indicated. (**C**) The P values for disease association, as determined by IPA (related to **Fig. 4c**). (**D**)-(**E**) Differentially expressed synaptic proteomes of ILA, as analyzed by Syngo (https://www.syngoportal.org). (**D**) The DEPs of male mutant mice vs. male wild-type mice. (**E**) The DEPs of female mutant mice vs. female wild-type mice. The up- and down-regulated DEPs are shown separately. These analyses are based on both the location (pre- and post-synapses) and the function of DEPs. The gene count for each analysis is also indicated in the upper left corner.

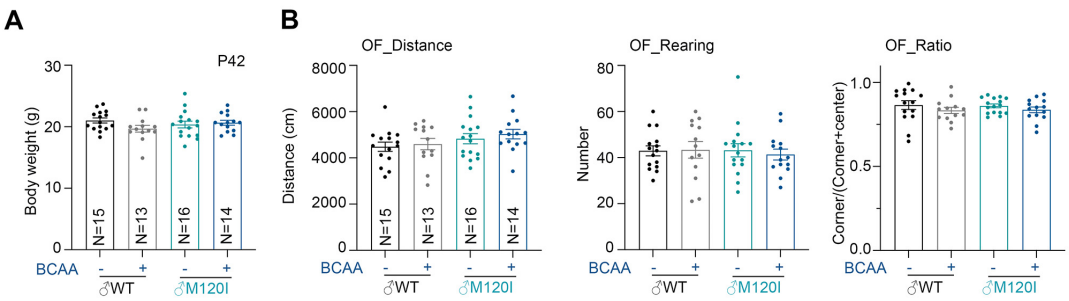

Supplementary Fig. 8. BCAA supplementation does not alter body weight or mouse behaviors in an open field (related to Fig. 5). (**A**) Body weight of mice after BCAA supplementation for 7 days at P42. (**B**) Mouse behaviors in an open field (OF). The same mice were used in Figure 5 and here. Total travel distance, numbers of rearing events, and the ratio of the time spent at corners to the sum of time spent at corners and center in an OF were measured 4 days after BCAA supplementation. None of the behavioral features in the open field were altered. Sample sizes (*N*, number of mice) are indicated. Data are presented as means ± SEM, and the results of individual mice are shown.

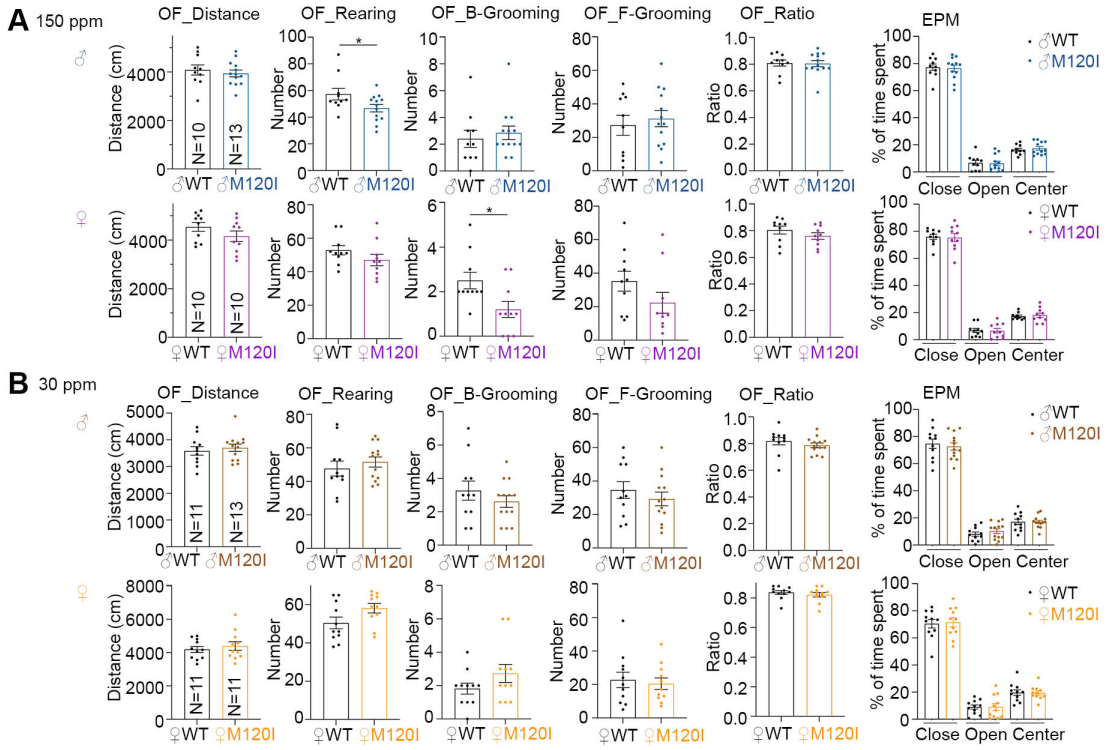

Supplementary Fig. 9. Zinc supplementation does not alter mouse behaviors in an open field or elevated plus maze (related to Fig. 6).

The same sets of mice with different intakes of zinc used in **Fig. 6** were also analyzed in an open field (OF) at P30 and in an elevated plus maze (EPM) test at P32, as indicated in **Fig. 6A**. The results are summarized here. (**A**) Mice fed 150 ppm zinc diet. (**B**) Mice fed 30 ppm zinc diet. Total travel distance, number of rearing events, number of face (F) and body (B) grooming events, and the ratio of the time spent at corners to the sum of time spent at corners and center in an OF were measured. The percentages of time spent in the closed arm, open arm and center area of the elevated plus maze are summarized in the right panel. None of the behavioral features in the open field or elevated plus maze were altered. The sample size (*N*, number of mice) is shown in the respective columns of the panel on the left. Data are presented as means ± SEM, and the results of individual mice are shown.

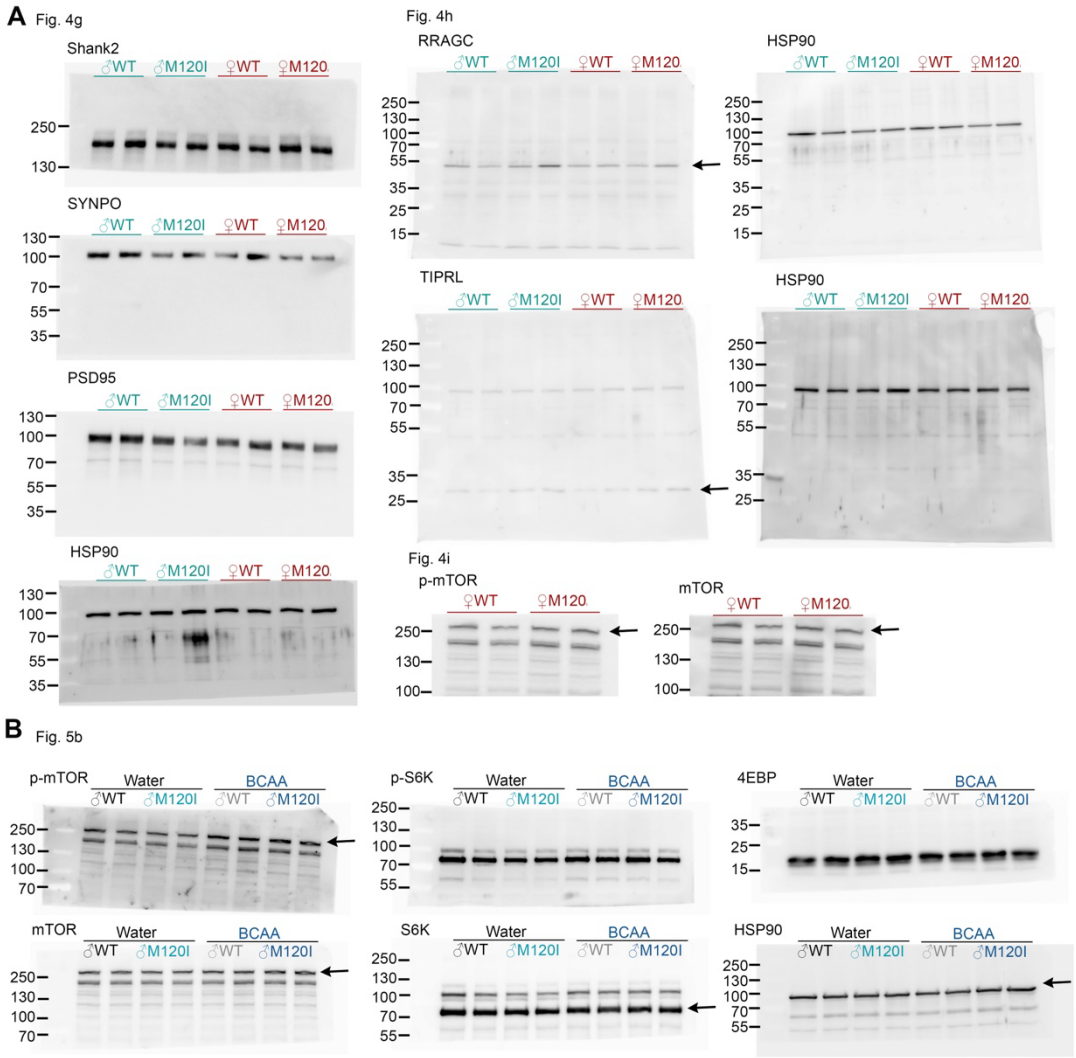

Supplementary Fig. 10. Uncropped images of all immunoblotting experiments presented in this report (related to Fig. 4 and 5). (**A**) Original blots of Fig. 4. **(B)** Original blots of Fig. 5.

Supplementary Methods

Open-field (OF) test

Mice were individually placed into the center of a transparent plastic box (40 x 40 x 32.5 cm) and allowed to freely explore the box for 10 min. Mouse behaviors in the box were video recorded from above and analyzed using the Smart Video Tracking System (Panlab, Barcelona, Spain). Total traveling distance (representing horizontal locomotion activity), number of rearing events (representing exploratory and vertical locomotion activity), number of grooming events and the ratio of time spent in the corners to the total time spent in the corners plus the central area (representing the degree of anxiety) were measured.

Light-dark box (LDB) test

A black box (19 x 39 x 45 cm) was inverted and put into the open field box to divide the space into two equal compartments. A small opening at the bottom of the black box (5 x 10 cm) allowed mice to freely explore the light and dark areas. Behaviors in the light-dark box were videotaped from above for 10 min. The time spent in the light box was analyzed using the Smart Video Tracking System (Panlab, Barcelona, Spain).

Elevated plus maze (EPM)

The apparatus raised to a height of 45.5 cm above the laboratory floor consisted of two open arms (30 cm x 5 cm), and two closed arms (30 cm x 5 cm) enclosed by 14 cm-high walls extending from a central platform (5 cm x 5 cm). An individual mouse was placed on the central area facing the open arm and allowed to freely explore the entire maze for 10 min. Movement was videotaped from above and analyzed using the Smart Video Tracking System (Panlab, Barelona, Spain). The percentage of time spent in the open arms, closed arms, and central area were determined. A higher percentage in the closed arm indicates a higher level of anxiety.

Three-chamber (3C) test

A transparent plastic box (17.5 x 41.5 x 22 cm) was divided into three equal compartments by means of two sliding doors. An identical cylindrical wire cage (16 cm in height, 9.5 cm in diameter) was placed individually inside each of the two side chambers. Directly before conducting the test, the test mice were placed into a new nesting cage. The entire test consisted of three 10-min sessions—i.e. habituation,

sociability, and novelty preference tests—with 2 min intervals between each session. Compartments and wire cages were cleaned with 75% EtOH and water after each task. During intervals, the test mice were placed back in the nesting cage. In the first habituation session, both cylindrical wire cages were empty. In the second sociability test, a plastic toy of a cartoon character of similar size to the adult mice was used as an inanimate object (Ob), which was randomly placed in the wire cage of either the left or right chamber. An unfamiliar mouse of the same sex and of similar size and age (S1) was placed in the other wire cage in the opposite chamber. In the last social novelty session, the inanimate object was replaced by another unfamiliar mouse (S2). The movement and sniffing behaviors of mice were recorded by videotaping from above. Sniffing toward the cylindrical wire cages was quantified manually without knowing the genotype of the mice. The total sniffing time was used to represent social interaction. The values of (T_{S1}-T_{Ob}) and (T_{S2}-T_{S1}) were determined as preference indices of sociability and social novelty, respectively.

Reciprocal social interaction (RSI) test

The lid of the home cage of test mice was removed to habituate mice for at least 5 min. WT C57BL/6J unfamiliar mice of the same sex and similar age and body weight were then introduced into the home cage of the test mice. Interactions were videotaped from above for 5 min. Time spent in social interactions, including sniffing, following and allogrooming, was recorded and analyzed blind to the genotype.

Magnetic resonance imaging

Mice were anesthetized and intracardially perfused with 10 ml of 0.1 M PBS containing 10 U/ml heparin, followed by 10 ml of 4% paraformaldehyde (PFA). The entire brain and skull were post-fixed in 4% PFA at 4 °C overnight and transferred to 0.1 M PBS and 0.02% sodium azide for at least one month before MRI scanning [1]. The solutions mentioned above all contained 2 mM ProHance. The anatomical MRI scans were performed using a T2-weighted, three-dimensional fast spin-echo sequence, with a cylindrical acquisition of k-space, and with a repetition time (TR) of 350 ms, echo time (TE) of 12 ms per echo for six echoes, a field of view of 20 × 20 × 25 mm^3, and a matrix size = 504 × 504 × 630 generating an image of 0.040 mm isotropic voxels. Total imaging time was ~ 14 h [2]. For the volume measurements, deformations encompassing the entire brain of each individual mouse were calculated in a common consensus space using deformation-based morphometry (DBM), which includes iterative linear and nonlinear

registrations. The Jacobian determinants of the deformation fields were then calculated as measures of volume for each voxel. Volume changes were additionally calculated by warping a pre-existing classified MRI atlas onto the population atlas, which allowed for the volume of 182 segmented structures [3-7]. These measurements could then be examined on a voxel-wise basis to localize the differences found within regions or across the brain. Multiple comparisons were accounted for using the false discovery rate (FDR).[8]

Immunofluorescence staining

Immunofluorescence staining of mouse brains was performed as described previously [9]. Mice were anesthetized and perfused with PBS followed by 4% paraformaldehyde in PBS. The mouse brains were cryopreserved in 30% sucrose solution at 4 ºC and embedded in OCT. We collected 50-µm-thick coronal sections using a cryostat microtome (CM1900, Leica). After washing with Tris-buffered saline (TBS), the brain sections were permeabilized with 0.1% Triton X-100 in TBS and blocked with 3% horse serum and 2% bovine serum albumin (BSA) in TBS at room temperature for 2 h. Primary antibodies were then added for overnight incubation at 4 ºC. After washing, brain sections were incubated with Alexa flour-488 and/or Alexa flour-555-conjugated secondary antibodies. Cell nuclei were counterstained with DAPI. Images were collected using an epifluorescence microscope (AxioImager-Z1; Carl Zeiss) or a confocal microscope (LSM700, Carl Zeiss) driven by Zen blue or Zen 2009, respectively.

Liquid chromatography-tandem mass spectrometry (LC-MS-MS) analysis

Preparation of the synaptosomal fraction of mouse brains

Synaptosomal fractions were prepared as described previously [10, 11] with some minor modifications. In brief, four biological repeats were used for each group. Given that the ILA is a very small brain region, the tissue samples of three mice were pooled as one replicate. The brains corresponding to section number 39-41 of Allen Brain Atlas were dissected and sliced into 300-µm-thick sections in ice-cold PBS using a vibratome (DTK-1000, Dosaka, Japan). The ILA regions were collected from each brain slice under a dissecting microscope and kept at -80 ºC before fractionation. The brain tissues were homogenized using a tissue Dounce homogenizer with a loose pestle in 300 µl sucrose buffer [50 mM Tris-Cl pH7.4, 320 mM sucrose, 2 mM DTT, 2 µm/ml leupeptin,

2 µm/ml pepstatin-A, 2 µm/ml aprotinin, 2 mM PMSF]. This total homogenate was centrifuged at 800 x *g* for 10 min at 4 ºC. The supernatant was collected and centrifuged again at 9200 x *g* for 15 min to collect the pellet as a crude synaptosomal fraction. Equal protein amounts of fractions were subjected to trypsinization and NanoLC-nanoESI-MS/MS analysis using an EASY-nLC 1200 system linked to a Thermo Orbitrap Fusion Lumos mass spectrometer (Thermo-Fisher Scientific, Bremen, Germany) equipped with a Nanospray Flex ion source (Thermo-Fisher Scientific, Bremen, Germany). Detailed methods are reported in our recent publications [10, 11].

Label-free quantification

Our proteomic data were searched against the Swiss-Prot *Mus musculus* database (17,049 entries total) using the Mascot search engine (v.2.6.2; Matrix Science, Boston, MA, USA) through Proteome Discoverer (v 2.2.0.388; Thermo-Fisher Scientific, Waltham, MA, USA). The search criteria were trypsin digestion, carbamidomethyl (C) for the fixed modification, oxidation (M) and acetylation (protein N-terminal) for the variable modifications, two missed cleavages, and 10 ppm of mass accuracy for the parent ion and 0.6 Da for the fragment ions. The false discovery rate (FDR) was calculated using the Proteome Discoverer Percolator function, and identifications with an FDR > 1% were rejected. For label-free quantification, precursor ion areas were extracted using the Minora Feature Detector node in Proteome Discoverer 2.2 with a 2-ppm mass precision and 2 min retention time-shift (to align the LC/MS-MS peaks mapping the isotope pattern and retention time). The ratios for each peptide were normalized against the total identified peptides and were used for protein-level quantification.

Analysis of functional protein networks and gene ontology

After quantifying the LC-MS-MS data, peptide signals of reliable quality and an adjusted *p*-value < 0.05 were used to identify differentially expressed proteins (**Supplementary Tables 4-5**). STRING analysis (version 11.0, https://string-db.org/) was employed to identify functional protein networks. Lines between nodes indicate that the interactions are based on experimental or STRING database evidence. The thickness of the lines indicates the confidence associated with the interaction. Different colors indicate associations with various gene ontology (GO), reactome (MMU) or annotated keyword (KW) pathways. Some nodes have multiple colors, indicating their involvement in multiple pathways.

References

1. de Guzman AE, Wong MD, Gleave JA, Nieman BJ. Variations in post-perfusion immersion fixation and storage alter MRI measurements of mouse brain morphometry. NeuroImage. 2016;142:687-95.
2. Spencer Noakes TL, Henkelman RM, Nieman BJ. Partitioning k-space for cylindrical three-dimensional rapid acquisition with relaxation enhancement imaging in the mouse brain. NMR in biomedicine. 2017;30(11).
3. Dorr AE, Lerch JP, Spring S, Kabani N, Henkelman RM. High resolution three-dimensional brain atlas using an average magnetic resonance image of 40 adult C57Bl/6J mice. Neuroimage. 2008;42(1):60-9.
4. Steadman PE, Ellegood J, Szulc KU, Turnbull DH, Joyner AL, Henkelman RM, et al. Genetic effects on cerebellar structure across mouse models of autism using a magnetic resonance imaging atlas. Autism research : official journal of the International Society for Autism Research. 2014;7(1):124-37.
5. Ullmann JF, Watson C, Janke AL, Kurniawan ND, Reutens DC. A segmentation protocol and MRI atlas of the C57BL/6J mouse neocortex. Neuroimage. 2013;78:196-203.
6. Beera KG, Li YQ, Dazai J, Stewart J, Egan S, Ahmed M, et al. Altered brain morphology after focal radiation reveals impact of off-target effects: implications for white matter development and neurogenesis. Neuro-oncology. 2018;20(6):788-98.
7. Qiu LR, Fernandes DJ, Szulc-Lerch KU, Dazai J, Nieman BJ, Turnbull DH, et al. Mouse MRI shows brain areas relatively larger in males emerge before those larger in females. Nature communications. 2018;9(1):2615.
8. Genovese CR, Lazar NA, Nichols T. Thresholding of statistical maps in functional neuroimaging using the false discovery rate. Neuroimage. 2002;15(4):870-8.
9. Huang TN, Yen TL, Qiu LR, Chuang HC, Lerch JP, Hsueh YP. Haploinsufficiency of autism causative gene Tbr1 impairs olfactory discrimination and neuronal activation of the olfactory system in mice. Molecular autism. 2019;10:5.
10. Shih PY, Hsieh BY, Lin MH, Huang TN, Tsai CY, Pong WL, et al. CTTNBP2 Controls Synaptic Expression of Zinc-Related Autism-Associated Proteins and Regulates Synapse Formation and Autism-like Behaviors. Cell reports. 2020;31(9):107700.
11. Shih YT, Huang TN, Hu HT, Yen TL, Hsueh YP. Vcp Overexpression and Leucine Supplementation Increase Protein Synthesis and Improve Fear Memory and Social Interaction of Nf1 Mutant Mice. Cell reports. 2020;31(13):107835.

Supplementary Table 1 Quantification results from structural MRI (sMRI) of male and female *Cttnbp2* M120I mice (related to Fig. 2).

Absolute Volumes	**M120I**		**WT**					
	Mean	**SD**	**Mean**	**SD**	**%Diff**	**Effect**	**P-value**	**FDR**
Amygdala	9.36	0.34	9.32	0.42	0.47	0.10	0.72	0.96
Anterior_commissure_pars_anterior	0.88	0.03	0.86	0.04	1.50	0.31	0.28	0.96
Anterior_commissure_pars_posterior	0.41	0.03	0.40	0.03	0.66	0.09	0.77	0.96
Basal_forebrain	5.36	0.18	5.37	0.20	-0.33	-0.09	0.76	0.96
Bed_nucleus_of_stria_terminalis	1.34	0.09	1.31	0.11	2.05	0.24	0.42	0.96
Cerebellar_peduncle_inferior	0.80	0.05	0.81	0.05	-0.93	-0.14	0.63	0.96
Cerebellar_peduncle_middle	1.19	0.05	1.19	0.06	-0.23	-0.05	0.87	0.96
Cerebellar_peduncle_superior	1.01	0.06	1.01	0.07	0.10	0.01	0.96	0.98
Cerebral_aqueduct	0.51	0.08	0.51	0.06	-0.55	-0.05	0.90	0.96
Cerebral_peduncle	1.99	0.08	2.00	0.08	-0.64	-0.16	0.62	0.96
Colliculus_inferior	5.48	0.28	5.46	0.33	0.22	0.04	0.90	0.96
Colliculus_superior	8.78	0.56	8.73	0.51	0.58	0.10	0.77	0.96
Corpus_callosum	11.12	0.55	11.10	0.72	0.24	0.04	0.90	0.96
Corticospinal_tract_pyramids	1.38	0.23	1.52	0.28	-9.47	-0.52	0.08	0.96
Cuneate_nucleus	0.24	0.04	0.24	0.04	-1.64	-0.09	0.76	0.96
Facial_nerve_cranial_nerve_7	0.22	0.02	0.22	0.02	1.15	0.12	0.68	0.96
Fasciculus_retroflexus	0.24	0.01	0.23	0.01	0.82	0.14	0.66	0.96
Fimbria	3.30	0.26	3.22	0.29	2.58	0.29	0.35	0.96
Fornix	0.64	0.03	0.63	0.03	0.98	0.19	0.51	0.96
Fourth_ventricle	0.89	0.10	0.90	0.14	-2.01	-0.13	0.63	0.96
Fundus_of_striatum	0.16	0.01	0.16	0.01	-0.02	0.00	0.99	0.99
Globus_pallidus	3.41	0.26	3.34	0.19	2.36	0.41	0.29	0.96
Habenular_commissure	0.04	0.01	0.04	0.01	1.41	0.05	0.85	0.96
Hypothalamus	10.60	0.34	10.56	0.37	0.37	0.11	0.73	0.96
Inferior_olivary_complex	0.34	0.05	0.36	0.05	-5.91	-0.43	0.18	0.96
Internal_capsule	3.24	0.15	3.15	0.19	2.77	0.47	0.11	0.96
Interpedunclar_nucleus	0.26	0.02	0.26	0.02	1.33	0.20	0.51	0.96
Lateral_olfactory_tract	1.35	0.05	1.34	0.06	0.67	0.14	0.62	0.96
Lateral_septum	3.17	0.21	3.10	0.20	1.97	0.31	0.34	0.96
Lateral_ventricle	4.27	0.90	4.14	0.64	2.92	0.19	0.63	0.96
Mammillary_bodies	0.45	0.03	0.47	0.04	-2.92	-0.35	0.23	0.96
Mammilothalamic_tract	0.24	0.01	0.24	0.01	0.45	0.08	0.80	0.96
Medial_lemniscus_medial Longitudinal_fasciculus	2.31	0.25	2.45	0.27	-5.59	-0.50	0.11	0.96
Medial_septum	1.22	0.05	1.22	0.05	0.16	0.04	0.89	0.96
Medulla	24.74	2.69	25.24	3.12	-1.95	-0.16	0.60	0.96
Midbrain	13.80	0.83	13.72	0.81	0.56	0.10	0.77	0.96
Nucleus_accumbens	4.20	0.21	4.13	0.21	1.76	0.35	0.28	0.96
Olfactory_peduncle	2.23	0.09	2.22	0.11	0.53	0.10	0.72	0.96
Olfactory_tubercle	3.26	0.31	3.35	0.36	-2.78	-0.26	0.39	0.96
Optic_tract	1.49	0.12	1.49	0.08	0.38	0.07	0.86	0.96
Periaqueductal_grey	3.96	0.24	3.93	0.24	0.87	0.14	0.66	0.96
Pons	16.84	0.55	16.82	0.57	0.13	0.04	0.90	0.96
Pontine_nucleus	0.74	0.06	0.74	0.05	1.01	0.15	0.66	0.96
Posterior_commissure	0.14	0.01	0.14	0.01	1.03	0.16	0.58	0.96
Pre_para_subiculum	2.27	0.16	2.26	0.09	0.52	0.13	0.78	0.96
Stria_medullaris	0.70	0.04	0.69	0.05	1.25	0.18	0.55	0.96
Stria_terminalis	0.95	0.05	0.94	0.06	0.99	0.15	0.59	0.96
Striatum	20.51	0.74	20.06	1.16	2.21	0.38	0.16	0.96
Subependymale_zone_rhinocele	0.04	0.00	0.04	0.00	3.75	0.59	0.06	0.96

Superior_olivary_complex	0.78	0.06	0.79	0.06	-0.30	-0.04	0.90	0.96
Thalamus	17.79	0.94	17.46	0.96	1.93	0.35	0.27	0.96
Third_ventricle	1.33	0.11	1.32	0.11	0.77	0.09	0.78	0.96
Ventral_tegmental_decussation	0.13	0.01	0.13	0.01	-0.29	-0.04	0.90	0.96
Lobules_1_2_lingula_and Central_lobule_ventral	1.56	0.14	1.56	0.15	0.17	0.02	0.95	0.98
Lobule_3_central_lobule_dorsal	1.88	0.14	1.87	0.20	0.48	0.05	0.87	0.96
Lobules_4_5_culmen_ventral And_dorsal	4.11	0.29	4.03	0.40	1.93	0.20	0.49	0.96
Lobule_6_declive	2.67	0.15	2.92	0.36	-8.71	-0.72	0.01	0.96
Lobule_7_tuber_or_folium	1.05	0.15	1.17	0.22	-10.31	-0.54	0.05	0.96
Lobule_8_pyramis	1.54	0.15	1.60	0.26	-3.90	-0.24	0.35	0.96
Lobule_9_uvula	2.76	0.18	2.79	0.39	-1.07	-0.08	0.76	0.96
Lobule_10_nodulus	1.24	0.12	1.21	0.23	3.06	0.16	0.54	0.96
Anterior_lobule_lobules_4_5	1.57	0.09	1.54	0.13	1.93	0.23	0.41	0.96
Simple_lobule_lobule_6	4.92	0.16	4.84	0.25	1.69	0.33	0.22	0.96
Crus_1_ansiform_lobule_lobule_6	4.26	0.18	4.30	0.28	-0.83	-0.13	0.64	0.96
Crus_2_ansiform_lobule_lobule_7	3.84	0.18	3.97	0.20	-3.05	-0.61	0.05	0.96
Paramedian_lobule_lobule_7	4.09	0.34	4.21	0.33	-2.68	-0.34	0.29	0.96
Copula_pyramis_lobule_8	2.35	0.17	2.38	0.16	-1.30	-0.19	0.56	0.96
Flocculus_FL	1.00	0.07	0.97	0.08	2.69	0.32	0.28	0.96
Paraflocculus_PFL	3.43	0.41	3.39	0.40	1.04	0.09	0.78	0.96
Trunk_of_arbor_vita	3.78	0.16	3.71	0.28	2.06	0.27	0.30	0.96
Lobule_1_2_white_matter	0.06	0.01	0.06	0.01	-1.31	-0.09	0.76	0.96
Lobule_3_white_matter	0.15	0.01	0.15	0.02	1.10	0.09	0.74	0.96
Trunk_of_lobules_1_3 White_matter	0.12	0.01	0.12	0.01	2.12	0.20	0.47	0.96
Lobules_4_5_white_matter	0.49	0.04	0.48	0.06	1.97	0.16	0.55	0.96
Lobules_6_7_white_matter	0.59	0.03	0.63	0.07	-5.40	-0.51	0.05	0.96
Lobule_8_white_matter	0.12	0.01	0.13	0.02	-4.19	-0.25	0.32	0.96
Trunk_of_lobules_6_8 White_matter	0.09	0.00	0.09	0.01	-2.58	-0.35	0.21	0.96
Lobule_9_white_matter	0.24	0.02	0.25	0.03	-1.52	-0.11	0.68	0.96
Lobule_10_white_matter	0.07	0.01	0.06	0.01	3.31	0.15	0.55	0.96
Anterior_lobule_white_matter	0.08	0.01	0.08	0.01	1.08	0.11	0.68	0.96
Simple_lobule_white_matter	0.35	0.02	0.33	0.02	3.65	0.50	0.07	0.96
Crus_1_white_matter	0.32	0.02	0.32	0.03	0.97	0.11	0.66	0.96
Trunk_of_simple_and_crus_1 White_matter	0.13	0.01	0.13	0.01	-0.63	-0.06	0.81	0.96
Crus_2_white_matter	0.22	0.01	0.22	0.02	-2.01	-0.27	0.36	0.96
Paramedian_lobule	0.13	0.01	0.13	0.01	-2.22	-0.20	0.46	0.96
Trunk_of_crus_2_and Paramedian_white_matter	0.27	0.02	0.28	0.02	-0.49	-0.06	0.83	0.96
Copula_white_matter	0.06	0.00	0.06	0.01	-0.99	-0.10	0.70	0.96
Paraflocculus_white_matter	0.25	0.02	0.25	0.02	-0.87	-0.12	0.72	0.96
Flocculus_white_matter	0.07	0.01	0.07	0.01	1.75	0.20	0.51	0.96
Dentate_nucleus	0.34	0.02	0.33	0.03	3.46	0.37	0.16	0.96
Nucleus_interpositus	0.44	0.03	0.43	0.04	1.96	0.20	0.45	0.96
Fastigial_nucleus	0.47	0.03	0.46	0.05	1.76	0.16	0.53	0.96
Cingulate_cortex_area_24a	1.95	0.17	1.97	0.12	-0.99	-0.16	0.67	0.96
Cingulate_cortex_area_24a.1	0.76	0.03	0.77	0.04	-0.51	-0.10	0.73	0.96
Cingulate_cortex_area_24b	1.74	0.14	1.72	0.11	1.58	0.25	0.50	0.96
Cingulate_cortex_area_24b.1	0.64	0.03	0.64	0.03	-0.06	-0.01	0.97	0.98
Cingulate_cortex_area_25	0.61	0.06	0.60	0.04	1.38	0.19	0.61	0.96
Cingulate_cortex_area_29a	0.71	0.05	0.71	0.06	-0.25	-0.03	0.91	0.97
Cingulate_cortex_area_29b	0.40	0.02	0.40	0.03	0.28	0.04	0.89	0.96

Cingulate_cortex_area_29c	1.92	0.09	1.91	0.09	0.46	0.09	0.76	0.96
Cingulate_cortex_area_30	2.85	0.19	2.85	0.15	-0.13	-0.03	0.94	0.98
Cingulate_cortex_area_32	2.62	0.30	2.59	0.21	1.27	0.15	0.69	0.96
Amygdalopiriform_transition_area	1.00	0.05	1.00	0.05	-0.48	-0.11	0.74	0.96
Primary_auditory_cortex	1.37	0.07	1.36	0.08	0.32	0.05	0.86	0.96
Secondary_auditory_cortex Dorsal_area	1.39	0.07	1.40	0.07	-0.15	-0.03	0.92	0.97
Secondary_auditory_cortex Ventral_area	1.56	0.12	1.55	0.12	0.35	0.05	0.88	0.96
Caudomedial_entorhinal_cortex	5.62	0.33	5.72	0.24	-1.72	-0.42	0.29	0.96
Cingulum	0.80	0.05	0.80	0.05	0.04	0.01	0.98	0.99
Claustrum	0.29	0.02	0.29	0.02	2.22	0.33	0.27	0.96
Cortex_amygdala_transition_zones	0.72	0.05	0.75	0.06	-4.67	-0.60	0.04	0.96
Claustrum_dorsal_part	0.25	0.02	0.25	0.02	1.33	0.17	0.56	0.96
Dorsal_nucleus_of The_endopiriform	1.41	0.12	1.39	0.12	1.89	0.22	0.49	0.96
Dorsal_intermediate Entorhinal_cortex	1.81	0.08	1.81	0.10	-0.32	-0.06	0.83	0.96
Dorsolateral_entorhinal_cortex	2.55	0.09	2.55	0.18	-0.12	-0.02	0.95	0.98
Dorsolateral_orbital_cortex	0.77	0.05	0.79	0.07	-2.76	-0.31	0.26	0.96
Dorsal_tenia_tecta	0.97	0.04	0.97	0.05	0.28	0.06	0.85	0.96
Ectorhinal_cortex	2.95	0.25	2.89	0.31	2.16	0.20	0.48	0.96
Frontal_cortex_area_3	0.73	0.04	0.74	0.04	-1.43	-0.24	0.44	0.96
Frontal_association_cortex	6.53	0.42	6.59	0.37	-0.99	-0.18	0.60	0.96
Intermediate_nucleus_of_the Endopiriform_claustrum	0.58	0.05	0.58	0.04	-0.11	-0.02	0.96	0.98
Insular_region_not_subdivided	7.53	0.50	7.58	0.54	-0.71	-0.10	0.75	0.96
Lateral_orbital_cortex	3.37	0.19	3.38	0.18	-0.35	-0.07	0.84	0.96
Lateral_parietal_association_cortex	0.24	0.02	0.24	0.02	-0.39	-0.05	0.87	0.96
Primary_motor_cortex	6.85	0.25	6.90	0.34	-0.69	-0.14	0.62	0.96
Secondary_motor_cortex	6.59	0.35	6.61	0.33	-0.26	-0.05	0.87	0.96
Medial_entorhinal_cortex	0.71	0.04	0.72	0.04	-1.22	-0.23	0.49	0.96
Medial_orbital_cortex	1.82	0.19	1.80	0.12	1.19	0.17	0.68	0.96
Medial_parietal_association_cortex	0.45	0.03	0.44	0.03	1.06	0.16	0.64	0.96
Piriform_cortex	10.09	0.54	10.03	0.41	0.58	0.14	0.70	0.96
Posterolateral_cortical Amygdaloid_area	0.87	0.05	0.89	0.05	-1.79	-0.32	0.34	0.96
Posteromedial_cortical Amygdaloid_area	1.06	0.07	1.07	0.06	-0.36	-0.06	0.85	0.96
Perirhinal_cortex	2.64	0.16	2.62	0.23	0.64	0.07	0.79	0.96
Parietal_cortex_posterior_area Rostral_part	0.13	0.01	0.13	0.01	-2.22	-0.37	0.23	0.96
Rostral_amygdalopiriform_area	0.42	0.03	0.43	0.03	-2.50	-0.38	0.25	0.96
Primary_somatosensory_cortex	4.11	0.28	4.17	0.22	-1.51	-0.28	0.44	0.96
Primary_somatosensory_cortex Barrel_field	9.25	0.50	9.35	0.55	-1.03	-0.17	0.56	0.96
Primary_somatosensory_cortex Dysgranular_zone	0.38	0.02	0.39	0.02	-1.60	-0.29	0.38	0.96
Primary_somatosensory_cortex Forelimb_region	3.94	0.24	3.99	0.23	-1.23	-0.21	0.51	0.96
Primary_somatosensory_cortex Hindlimb_region	2.80	0.14	2.82	0.13	-0.68	-0.15	0.66	0.96
Primary_somatosensory_cortex Jaw_region	0.61	0.06	0.62	0.05	-1.98	-0.24	0.49	0.96
Primary_somatosensory_cortex Shoulder_region	0.20	0.01	0.20	0.01	-0.24	-0.06	0.89	0.96

Primary_somatosensory_cortex Trunk_region	0.52	0.03	0.52	0.04	-0.75	-0.11	0.69	0.96
Primary_somatosensory_cortex Upper_lip_region	5.51	0.32	5.57	0.41	-1.20	-0.16	0.57	0.96
Secondary_somatosensory_cortex	7.02	0.58	7.07	0.46	-0.71	-0.11	0.76	0.96
Temporal_association_area	2.96	0.22	2.90	0.25	1.89	0.22	0.47	0.96
Primary_visual_cortex	2.37	0.16	2.40	0.18	-1.39	-0.18	0.54	0.96
Primary_visual_cortex_binocular Area	2.00	0.13	2.02	0.14	-1.00	-0.15	0.64	0.96
Primary_visual_cortex_monocular Area	1.89	0.15	1.91	0.12	-0.95	-0.16	0.67	0.96
Secondary_visual_cortex_lateral Area	2.74	0.16	2.74	0.20	0.04	0.01	0.99	0.99
Secondary_visual_cortex_mediolateral Area	1.04	0.10	1.03	0.08	0.41	0.05	0.88	0.96
Secondary_visual_cortex_mediomedial Area	1.74	0.14	1.73	0.14	0.44	0.05	0.87	0.96
Claustrum_ventral_part	0.54	0.03	0.53	0.04	1.61	0.23	0.42	0.96
Ventral_nucleus_of_the_endopiriform Claustrum	0.45	0.03	0.44	0.02	2.25	0.47	0.21	0.96
Ventral_intermediate_entorhinal_cortex	1.05	0.05	1.06	0.06	-0.75	-0.14	0.65	0.96
Ventral_orbital_cortex	1.50	0.10	1.51	0.08	-0.33	-0.06	0.87	0.96
Ventral_tenia_tecta	0.10	0.01	0.10	0.01	-2.96	-0.38	0.24	0.96
Ca10r	2.03	0.10	2.00	0.13	1.47	0.23	0.43	0.96
Lmol	2.34	0.12	2.32	0.10	0.83	0.20	0.58	0.96
Ca1rad	2.61	0.12	2.57	0.13	1.49	0.30	0.34	0.96
Ca2py	0.19	0.01	0.18	0.01	2.91	0.38	0.21	0.96
Ca20r	0.47	0.03	0.46	0.03	2.21	0.30	0.34	0.96
Ca2rad	0.47	0.03	0.46	0.03	2.41	0.36	0.24	0.96
Ca3py_inner	0.15	0.01	0.15	0.01	2.23	0.42	0.22	0.96
Ca3py_outer	1.01	0.11	0.97	0.06	4.00	0.63	0.16	0.96
Ca30r	2.85	0.36	2.77	0.17	3.02	0.48	0.36	0.96
Ca3rad	1.85	0.15	1.79	0.10	3.58	0.67	0.11	0.96
Slu	0.76	0.07	0.73	0.04	3.79	0.63	0.14	0.96
Modg	4.12	0.25	4.04	0.21	2.10	0.40	0.26	0.96
Grdg	1.29	0.08	1.25	0.06	3.04	0.61	0.10	0.96
Podg	0.63	0.04	0.61	0.03	2.67	0.50	0.14	0.96
Ca1py	1.11	0.06	1.09	0.07	2.10	0.33	0.27	0.96
Olfactory_bulb_glomerular_layer	4.25	0.22	4.28	0.24	-0.69	-0.12	0.69	0.96
Olfactory_bulb_external Plexiform_layer	6.46	0.24	6.41	0.31	0.76	0.15	0.59	0.96
Olfactory_bulb_mitral_cell_layer	1.29	0.04	1.26	0.06	2.10	0.48	0.10	0.96
Olfactory_bulb_internal Plexiform_layer	1.12	0.04	1.09	0.05	2.57	0.59	0.05	0.96
Olfactory_bulb_granule_cell_layer	4.64	0.15	4.49	0.19	3.27	0.75	0.01	0.96
Accessory_olfactory_bulb Glomerular_external_plexiform And_mitral_cell_layer	0.50	0.03	0.49	0.02	1.18	0.25	0.47	0.96
Accessory_olfactory_bulb Granule_cell_layer	0.25	0.02	0.24	0.02	3.84	0.59	0.14	0.96
Anterior_olfactory_nucleus	2.04	0.08	1.99	0.10	2.04	0.40	0.17	0.96
Subiculum	3.25	0.17	3.21	0.17	1.31	0.24	0.44	0.96
Medial_amygdala	1.09	0.06	1.09	0.07	-0.50	-0.08	0.78	0.96
Medial_preoptic_nucleus	0.21	0.01	0.21	0.01	0.69	0.10	0.76	0.96
Brain volumes	441.19	12.50	440.55	13.81	0.15	0.05	0.88	

Supplementary Table 2 List of brain regions subjected to C-FOS staining and the *P* values for the comparisons among four groups (related to Fig. 2).

Brain regions	Abbr.	P values of each comparison of C-FOS+ cell No.				Atlas Section No.
		♂M120I:♂WT	♀M120I:♀WT	♀WT: ♂WT	♀M120I:♂M120I	
Cortical regions						
mPFC-Prelimbic area	PL	0.2756	0.5962	0.6079	0.009**↑	41
mPFC-Infralimbic area	ILA	0.0135*↓	0.0709	0.1672	0.0134*↑	39
Anterior cingulate area, dorsal	ACAd	0.9215	0.9286	0.2049	0.2616	41
Anterior cingulate area, ventral	ACAv	0.5965	0.7435	0.2757	0.6262	44
Endopiriform nucleus	EPd	0.6582	0.3547	0.3529	0.5926	44
Piriform cortex	PIR	0.7557	0.8429	0.5947	0.9207	44
Retrosplenial area, dorsal	RSPd	0.9838	0.9999	0.5242	0.6306	70
Retrosplenial area, ventral	RSPv	0.796	0.7007	0.5725	0.5714	70
Primary motor area	Mop	0.7134	0.9972	0.0742	0.289	70
Secondary motor area	Mos	0.7424	0.4809	0.0784	0.2582	70
Pallidum regions						
Lateral septal nucleus, rotral	LSr	0.0488*↓	0.8	0.502	0.4535	48
Medial septal nucleus	MS	0.0114*↓	0.2439	0.5024	0.0532	48
Caudoputmen	CP	0.297	0.5683	0.3904	0.5141	48
Bed nuclei of the stria terminalis, anteriomedial	BSTam	0.0119*↓	0.6237	0.3371	0.0401*↑	48
Nucleus accumbens	ACB	0.6323	0.6769	0.4298	0.0603	44
Taenia tecta, dorsal part	TTd	0.1089	0.6014	0.8614	0.0859	41
Hippocampus regions						
Dorsal CA1	CA1d	0.902	0.9846	0.5251	0.5776	70
Dorsal CA3	CA3d	0.1114	0.9697	0.8633	0.1081	70
Denta gyrus, dorsal	DGd	0.0136*↓	0.5402	0.6744	0.027*↑	70
Ventral CA1	CA1v	0.233	0.9171	0.3321	0.0852	82
Ventral subiculum	SUBv	0.0592	0.1192	0.1601	0.3004	82
Thalamus/Hyppthalamus regions						
Lateral Habenula	LH	0.5196	0.044*↓	0.3059	0.7519	68
Mediodorsal nucleus of thalamus	MD	0.7461	0.9151	0.8355	0.7662	68
Paraventricular nucleus of the thalamus	PVT	0.0543	0.7234	0.0469*↓	0.7862	68
Dorsomedial nucleus of the hypothalamus	DMH	0.0791	0.758	0.0717	0.9589	68
Ventromedial hypothalamic nucleus	VMH	0.219	0.8746	0.822	0.1881	68
Amygdala regions						
Medial amygdala, ventral	MEAav	0.7948	0.7511	0.8579	0.471	70
Medial amygdala, dorsal	MEAad	0.0931	0.6533	0.9874	0.0556	70
Lateral amygdala	LA	0.7352	0.0384*↑	0.8454	0.0947	73
Basolateral amygdala	BLAa	0.0019**↓	0.9818	0.6752	0.0044**↑	70
Midbrain regions						
Ventral tegmental area	VTA	0.0081**↓	0.8432	0.6787	0.0291*↑	82

*, $P < 0.05$; **, $P < 0.01$.

Supplementary Table 3 The ratios of mean C-FOS+ cell density across 31 brain regions (related to Fig. 2A).

Brain regions	Abbr.	C-FOS+ cell No./mm2 ♂WT/♂M120I	♀WT/♀M120I	Atlas Section No.
Cortical regions				
mPFC-Prelimbic area	PL	640.4/632.7	696/839.5	39
mPFC-Infralimbic area	ILA	584.5/373.7*	437.6/708.6	39
Anterior cingulate area, dorsal	ACAd	438.4/449.4	608.4/624	41
Anterior cingulate area, ventral	ACAv	650.4/721.3	869/796.9	44
Endopiriform nucleus	EPd	353.1/387.5	448.7/339	44
Piriform cortex	PIR	806/867.9	938.9/888	44
Retrosplenial area, dorsal	RSPd	635.2/631.6	751/751.1	70
Retrosplenial area, ventral	RSPv	723.8/677.1	867.6/770.5	70
Primary motor area	Mop	411.3/467.7	690.4/689.7	70
Secondary motor area	Mos	495.4/465.6	784.1/640.1	70
Pallidum regions				
Lateral septal nucleus, rotral	LSr	307.3/194	258.6/291.4	44
Medial septal nucleus	MS	204.9/148	243.7/272.9	44
Caudoputmen	CP	45.19/45.32	68.58/62.18	44
Bed nuclei of he stria terminalis, anteriomedial	BSTam	362.6/191**	297.5/331.8	48
Nucleus accumbens	ACB	140.9/124.3	175.2/193.3	44
Taenia tecta, dorsal part	TTd	242.9/163.8	232.1/272.1	41
Hippocampus regions				
Dorsal CA1	CA1d	177.8/191.8	269.8/266.6	70
Dorsal CA3	CA3d	619.5/444.3	644/650.1	70
Denta gyrus, dorsal	DGd	450.9/280*	416/476.7	70
Ventral CA1	CA1v	316.9/268.5	378.3/387.2	82
Ventral subiculum	SUBv	287.5/194.2	360.3/256.4	86
Thalamus / Hyppthalamus regions				
Lateral Habenula	LH	503.2/410.4	685.4/382.9*	68
Mediodorsal nucleus of thalamus	MD	179.2/117.9	193.2/177.5	70
Paraventricular nucleus of the thalamus	PVT	856.9/686.3	868.4/817	70
Dorsomedial nucleus of the hypothalamus	DMH	543.6/354.7	401.2/444.2	70
Ventromedial hypothalamic nucleus	VMH	135.2/58.48*	111.4/102.1	70
Amygdala regions				
Medial amygdala, ventral	MEAav	222.7/197	240.7/275.3	70
Medial amygdala, dorsal	MEAad	304.4/192.6	305.5/341.7	70
Lateral amygdala	LA	340.9/359.6	330.5/482.4*	73
Basolateral amygdala, anterior	BLAa	374.5/206.1***	353.9/352.8	70
Midbrain regions				
Ventral tegmental area	VTA	187.9/96.48**	201.5/211.7	82

*, $P < 0.05$; **, $P < 0.01$; ***, $P < 0.001$.

Supplementary Table 4 Differentially expressed proteins in ILA synaptic proteomes between male M120I mutant and male wild-type mice (related to Fig. 4).

DEPs of male M120 vs. male WT				
Accession	Gene Symbol	Coverage [%]	Abundance Ratio: (MH) / (MW)	Abundance Ratio Adj. P-Value: (MH) / (MW)
O08644	Ephb6	10	0.037	2.52E-16
Q80TA1	Ept1; Selenoi	10	0.349	0.00230214
P63082	Atp6v0c; Atp6v0c-ps2	54	0.375	9.46E-14
O35683	Ndufa1	17	0.386	1.09E-12
Q9CYR0	Ssbp1	20	0.411	0.002306137
Q8BSL7	Arf2	59	0.445	0.023533662
Q9D7J4	Cox20; Fam36a	41	0.45	0.000271368
Q6NZC7	Sec23ip	5	0.485	0.008629853
Q3TC33	Ccdc127	30	0.491	0.000142533
Q9WTP6	Ak2	25	0.5	0.002543283
P0DN34	Ndufb1 , LOC102631912	54	0.503	3.04E-07
Q8BX17	Gemin5	2	0.506	2.77E-05
P00405	COX2	63	0.516	7.34E-07
Q7TNS2	Minos1	63	0.516	4.24E-07
P63137	Gabrb2	16	0.527	0.007047227
O35343	Kpna4	28	0.537	0.009786457
Q9JI91	Actn2	56	0.538	3.52E-06
Q60771	Cldn11	26	0.559	1.15E-05
P68033	Actc1	62	0.573	4.40E-05
P56391	Cox6b1	80	0.574	4.59E-05
P20917	Mag	20	0.575	6.59E-05
P03893	ND2	15	0.58	0.003984846
Q8C460	Eri3	9	0.58	0.013933869
P07310	Ckm	10	0.586	0.023005161
Q9CR21	Ndufab1	15	0.587	0.001973723
Q3UIU2	Ndufb6	70	0.591	0.000559492
Q9CQ91	Ndufa3	50	0.601	0.000397039
Q9CXZ1	Ndufs4	53	0.607	0.001000742
Q9CPX8	Uqcr11	64	0.617	0.000984048
Q9CQJ8	Ndufb9	75	0.623	0.000691021
Q8BIG7	Comtd1	50	0.634	0.00197541 1
Q8R3R8	Gabarapl1	26	0.642	0.016311935
Q7TPR4	Actn1	83	0.643	0.001735599
Q61885	Mog	39	0.646	0.002418096
Q8CC35	Synpo	50	0.666	0.006040417
Q3UTJ2	Sorbs2	31	0.673	0.005564212
Q9DCZ4	Apoo	67	0.679	0.015616574
B9EJA2	Cttnbp2	7	0.68	0.015616574
Q62108	Dlg4	63	0.684	0.009465882
Q9DC70	Ndufs7	54	0.691	0.02158813
F6SEU4	Syngap1	69	0.694	0.01366126
Q80Z38	Shank2	44	0.698	0.007899757
Q9D2R6	Coa3	27	0.699	0.015616574
Q9QZD9	Eif3i	51	1.567	0.042851124
P83882	Rpl36al; Rpl36a; Rpl36a-ps3	25	1.572	0.048017343

O55142	Rpl35a-ps4; Rpl35a; Rpl35a-ps2; Gm10243; Rpl35a-ps5; LOC100862595; Gm14279; LOC100048620	38	1.625	0.046561585
P35803	Gpm6b	34	1.63	0.038156786
P54227	Stmn1	58	1.658	0.036548924
Q3TTY5	Krt2	10	1.692	0.021894076
O35286	Dhx15	6	1.703	0.014132585
Q9D1R9	Rpl34-ps1; Rpl34; Gm4705	38	1.721	0.015616574
P61514	Rpl37a	67	1.735	0.011187981
Q3UV17	Krt76	10	1.744	0.015074469
Q62093	Srsf2	19	1.751	0.002457092
Q9R0Q3	Tmed2; Gm21540; LOC100862175; Gm10698	23	1.78	0.014185915
Q9CQE7	Ergic3	13	1.78	0.00411631
P61222	Abce1	9	1.798	0.024007321
P60761	Nrgn	60	1.825	0.001735599
Q8BXR1	Slc7a14	16	1.837	0.000574087
O89084	Pde4a	9	1.862	0.049290456
Q8BGD9	Eif4b	19	1.894	0.0006060l
Q9CT10	Ranbp3	19	1.986	0.023834652
P10922	H1f0	21	2.002	4.22E-05
Q3TMP8	Tmem38a	14	2.029	0.014527027
Q9Z204	Hnrnpc	12	2.172	0.001669241
Q9DB75	Cdip1	14	2.64	0.000545637
E9Q735	Ube4a	9	3.511	2.52E-16
Q64735	Cr1l	12	48.126	2.52182E-16

Supplementary Table 5 Differentially expressed proteins in ILA synaptic proteomes between female M120I mutant and female wild-type mice (related to Fig. 4).

DEPs of female M120I vs. female WT				
Accession	Gene Symbol	Coverage [%]	Abundance Ratio: (FH) / (FW)	Abundance Ratio Adj. P-Value: (FH) / (FW)
O09126	Sema4d	10	0.001	1.18802E-16
P61622	Itga11	2	0.013	1.18802E-16
P63143	Kcnab1	25	0.039	1.18802E-16
P63082	Atp6v0c; Atp6v0c-ps2	54	0.043	1.18802E-16
P00405	COX2	63	0.147	1.18802E-16
Q8C5W0	Clmn	9	0.149	6.10035E-06
Q9CPX8	Uqcr11	64	0.207	1.18802E-16
Q9R0Q3	Tmed2; Gm21540; LOC100862175; Gm10698	25	0.235	1.97797E-11
Q8R1T1	Chmp7	13	0.241	0.013851368
Q9JKK8	Atr	1	0.27	2.12072E-12
Q9CYN2	Spcs2	27	0.3	0.000353441
P03888	ND1	15	0.307	4.3806E-13
P47743	Grm8	8	0.313	0.001303942
Q91YH5	Atl3	25	0.315	0.002298174
Q91VW3	Sh3bgrl3	22	0.316	4.59475E-07
Q9ERS2	Ndufa13	67	0.318	8.02055E-10
Q7TNS2	Minos1	53	0.322	3.37472E-09
Q8BGZ1	Hpcal4	90	0.326	2.41198E-13
Q924M7	Mpi	39	0.335	0.001224408
Q04899	Cdk18	19	0.338	0.023384464
Q8K3J1	Ndufs8	51	0.352	2.45271E-09
Q9D8S4	Rexo2	17	0.36	0.000938889
P56391	Cox6b1	80	0.365	8.82735E-08
Q9CQ91	Ndufa3	50	0.369	3.1217E-07
Q922F4	Tubb6	48	0.373	1.87681E-07
Q9JM14	Nt5c	39	0.375	9.46696E-07
Q99K10	Nlgn1	13	0.381	0.001850105
Q9WTT4	Atp6v1g2	76	0.387	1.32879E-07
Q8BFZ3	Actbl2	60	0.388	1.935E-06
P03911	ND4	22	0.393	1.51841E-08
P56959	Fus	17	0.395	3.89875E-05
Q8BFY6	Pef1	20	0.398	0.003097794
P03893	ND2	15	0.399	0.000567904
Q9CQJ8	Ndufb9	75	0.4	1.54759E-06
Q9CQZ6	Ndufb3	35	0.429	2.37058E-07
Q9DB10	1500032L24Rik; Smdt1	51	0.431	2.50971E-05
O35972	Mrpl23; Mrpl23-ps1	17	0.432	0.038016273

P62823	Rab3c	56	0.435	1.64095E-05
P70392	Rasgrf2	17	0.441	8.90654E-05
P12815	Pdcd6	51	0.444	3.44459E-05
P29387	Gnb4	71	0.458	4.0065E-06
O88967	Yme1l1	8	0.462	0.010078828
P63216	Gng3	84	0.463	3.68853E-05
Q9JL26	Fmnl1	5	0.464	0.04869973
P68372	Tubb4b	80	0.475	0.000156708
Q9CPQ3	Tomm22	66	0.475	7.72991E-05
P48771	Cox7a2	60	0.477	3.44459E-05
Q8BHL3	Tbc1d10b	26	0.479	0.001984545
P21460	Cst3	45	0.481	0.000206924
Q5M8N0	Cnrip1	77	0.487	0.000299139
Q8BMP6	Acbd3	27	0.49	0.025095345
Q9CQ69	Uqcrq	80	0.491	0.000358226
O09167	Rpl21	33	0.493	2.90414E-05
Q9ERD7	Tubb3	82	0.505	0.000670343
Q3UIU2	Ndufb6	80	0.509	0.000216884
P20917	Mag	21	0.51	0.000575635
P70699	Gaa	25	0.511	0.00086395
O08529	Capn2	27	0.515	0.019177034
Q6P4S6	Sik3	7	0.516	0.044474514
P56480	Atp5b	82	0.531	0.001986489
Q9CQ85	Timm22	31	0.533	0.002219517
Q91YX5	Lpgat1	29	0.541	0.002931225
Q7TMM9	Tubb2a	85	0.545	0.003436721
Q9CRA5	Golph3	28	0.547	0.006579528
Q80VP9	Asphd2	38	0.549	0.015716548
P26883	Fkbp1a	46	0.557	0.000543954
Q9QXX4	Slc25a13	8	0.571	0.000660933
Q8BG67	Efr3a	17	0.573	0.048065096
Q6NS82	Fam134a; Retreg2	15	0.575	0.019476187
Q9DCS9	Ndufb10	64	0.577	0.010133652
P43274	Hist1h1e	26	0.578	0.019014589
Q60771	Cldn11	43	0.578	0.001910945
Q9CXV1	Sdhd	28	0.58	0.004939999
Q61335	Bcap31	31	0.581	0.020281428
Q91XV3	Basp1	94	0.583	0.012377759
P63330	Ppp2ca	75	0.586	0.023987164
Q9CXZ1	Ndufs4	53	0.588	0.006146643
Q62283	Tspan7	18	0.591	0.004939999
Q9D1G1	Rab1b	69	0.594	0.003063448
Q80V26	Impad1	28	0.6	0.024957973
Q8BGN3	Enpp6	25	0.61	0.027039968

Q9QZB0	Rgs17	46	0.614	0.031229385
Q6DFY8	Brinp2; Fam5b	13	0.614	0.027707668
Q8VCD6	Reep2	28	0.616	0.035314337
Q91WD5	Ndufs2	75	0.617	0.032936418
Q9D855	Uqcrb	59	0.619	0.034079545
Q8VEH3	Arl8a	68	0.62	0.041359322
Q9D0R2	Tars	17	0.62	0.015377939
Q9CPQ8	Atp5l	71	0.623	0.038062755
Q8R164	Bphl	43	0.625	0.023274899
Q9JKL4	Ndufaf3	35	0.627	0.042877446
Q3UUI3	Them4	34	0.63	0.009511258
P55096	Abcd3	33	0.631	0.041340881
Q8R404	2410015M20Rik	72	0.638	0.013671075
Q9EPJ9	Arfgap1	69	0.652	0.037797986
Q9DBE8	Alg2	51	0.654	0.023274899
Q99JI6	Rap1b	82	0.655	0.017506862
P04925	Prnp	52	0.663	0.04238861
P08551	Nefl	58	0.668	0.04631721
O70435	Psma3	37	1.671	0.035705029
P09528	Fth1	57	1.692	0.028777433
P99026	Psmb4	48	1.719	0.042448959
P08228	Sod1	88	1.731	0.035705029
P01942	Hba-a1; Hba-a2	70	1.781	0.023987164
Q61016	Gng7	72	1.781	0.023987164
Q3TCJ1	Fam175b; Abraxas2	6	1.803	0.043475802
Q99K70	Rragc	40	1.812	0.019476187
O55100	Syngr1	18	1.828	0.015317184
Q5XG73	Acbd5	4	1.859	0.010751721
Q7SIG6	Asap2	13	1.878	0.00942027
Q6IFX2	Krt42	26	1.98	0.003346272
P97450	Atp5j	31	2.146	0.024003019
Q61781	Krt14	27	2.191	0.000146515
Q3UV17	Krt76	8	2.211	0.000272019
P70236	Map2k6	11	2.239	0.049316736
Q8BH58	Tiprl	15	2.309	0.01382927
Q8QZV4	Stk32c	24	2.343	0.035015635
P60761	Nrgn	60	2.389	2.12247E-05
Q922U2	Krt5	24	2.457	2.12247E-05
P04104	Krt1	6	2.611	3.93323E-06
Q8VED5	Krt79	9	2.682	6.25171E-08
Q3TTY5	Krt2	10	2.7	1.47974E-06
O88735	Map7; Mtap7	3	2.807	2.48552E-06
Q6Y685	Tacc1	3	2.964	0.003971802
Q91YW3	Dnajc3	12	3.005	3.38438E-09

Q6IFZ6	Krt77	14	3.07	2.59696E-08
Q3V132	Slc25a31	13	3.359	2.25301E-09
P02535	Krt10	15	3.499	2.65044E-10

Supplementary Table 6 Disease associations of female differentially expressed proteins in ILA synaptic proteomes (related to Fig. 4).

Protein	Function (from STRING)	Disease Association	Reference (PMID or DOI)
NRGN	Neurogranin; Acts as a "third messenger" substrate of protein kinase C-mediated molecular cascades during synaptic development and remodeling.	Schizophrenia	33032807
SOD1	Superoxide dismutase [Cu-Zn]; Destroys radicals which are normally produced within the cells and which are toxic to biological systems.	Autism Spectrum Disorder	24155217, 28469396
DNAJC3 (HSP40)	DnaJ homolog subfamily C member 3; Involved in the unfolded protein response (UPR) during endoplasmic reticulum (ER) stress. Acts as a negative regulator of the EIF2AK4/GCN2 kinase activity by preventing the phosphorylation of eIF-2-alpha at 'Ser-52' and hence attenuating general protein synthesis under ER stress, hypothermic and amino acid starving stress conditions (By similarity). Co-chaperone of HSPA8/HSC70, it stimulates its ATPase activity.	Developmental delay	https://doi.org/10.1159/000358538
TIPRL	TIP41-like protein; May be a allosteric regulator of serine/threonine- protein phosphatase 2A (PP2A). Isoform 1 inhibits catalytic activity of the PP2A(D) core complex in vitro. The PP2A(C):TIPRL complex does not show phosphatase activity. Acts as negative regulator of serine/threonine-protein phosphatase 4 probably by inhibiting the formation of the active PPP4C:PPP4R2 complex.	(regulate mTOR pathway)	
RRAGC	Ras-related GTP-binding protein C; Guanine nucleotide-binding protein forming heterodimeric Rag complexes required for the amino acid-induced relocalization of mTORC1 to the lysosomes and its subsequent activation by the GTPase RHEB. This is a crucial step in the activation of the TOR signaling cascade by amino acids.	Autism Spectrum Disorder (regulate mTOR pathway)	29875476
MAP7	Ensconsin; Microtubule-stabilizing protein that may play an important role during reorganization of microtubules during polarization and differentiation of epithelial cells. Associates with microtubules in a dynamic manner. May play a role in the formation of intercellular contacts. Colocalization with TRPV4 results in the redistribution of TRPV4 toward the membrane and may link cytoskeletal microfilaments.	Schizophrenia	20371615
FTH1	Ferritin heavy chain; Stores iron in a soluble, non-toxic, readily available form. Important for iron homeostasis. Has ferroxidase activity. Iron is taken up in the ferrous form and deposited as ferric hydroxides after oxidation. Also plays a role in delivery of iron to cells.	Autism Spectrum Disorder	28469396
MAP2K6	Dual specificity mitogen-activated protein kinase kinase 6; Dual specificity protein kinase which acts as an essential component of the MAP kinase signal transduction pathway. With MAP3K3/MKK3, catalyzes the concomitant phosphorylation of a threonine and a tyrosine residue in the MAP kinases p38 MAPK11, MAPK12, MAPK13 and MAPK14 and plays an important role in the regulation of cellular responses to cytokines and all kinds of stresses. Especially, MAP2K3/MKK3 and MAP2K6/MKK6 are both essential for the activation of MAPK11 and MAPK13 induced by environmental stress.	Autism Spectrum Disorder	27842596, https://doi.org/10.1101/209908

Supplementary Table 7 Statistical methods and results (related to Fig. 1, 3, 4, 5 and 6).

Figure	Method	Group	Mean diff.	95.00% CI of diff.	P vale
Fig. 1B 3C_sociability; Male	Interaction times; Two-way ANOVA; Tukey's HSD multiple comparison test	+/+: S1 vs O	191.1	155.8 to 226.3	P<0.0001, ****
		+/-: S1 vs O	82.62	46.03 to 119.2	P<0.0001, ****
		-/-: S1 vs O	108.2	71.65 to 144.8	P<0.0001, ****
		S1: +/+ vs +/-	93.49	57.57 to 129.4	P<0.0001, ****
		S1: +/+ vs -/-	81.49	45.57 to 117.4	P<0.0001, ****
	Preference; Ordinary one-way ANOVA; Dunnett's. comparison test	+/+ vs +/-	108.5	70.83 to 146.1	P<0.0001, ****
		+/+ vs -/-	82.84	45.21 to 120.5	P<0.0001, ****
Fig 1B 3C_sociability; female	Interaction times; Two-way ANOVA; Tukey's HSD multiple comparison test	+/+: S1 vs O	200.1	150.7 to 249.6	P<0.0001, ****
		+/-: S1 vs O	179.3	134.4 to 224.1	P<0.0001, ****
		-/-: S1 vs O	193.6	137.9 to 249.4	P<0.0001, ****
	Preference; Ordinary one-way ANOVA; Dunnett's. comparison test	+/+ vs +/-	20.85	-32.78 to 74.48	P=0.5798, ns
		+/+ vs -/-	-10.68	-70.54 to 49.19	P=0.8864, ns
Fig. 1B 3C_novelty preference; Male	Interaction times; Two-way ANOVA; Tukey's HSD multiple comparison test	+/+: S1 vs S2	94.43	52.14 to 136.7	P<0.0001, ****
		+/-:S1 vs S2	41.92	-1.963 to 85.81	P=0.0695, ns
		-/-:S1 vs S2	29.92	-13.96 to 73.81	P=0.3552, ns
		S2: +/+ vs +/-	41.46	-1.640 to 84.55	P=0.0662, ns
		S2: +/+ vs -/-	52.3	9.207 to 95.40	P=0.0085, **
	Preference; Ordinary one-way ANOVA; Dunnett's. comparison test	+/+ vs +/-	52.51	12.99 to 92.02	P=0.0079, **
		+/+ vs -/-	69.12	29.60 to 108.6	P=0.0005, ***
Fig. 1B 3C_novelty preference; Female	Interaction time; Two-way ANOVA; Tukey's HSD multiple comparison test	+/+: S1 vs S2	105.6	42.73 to 168.4	P<0.0001, ****
		+/-: S1 vs S2	107.6	50.56 to 164.6	P<0.0001, ****
		-/-: S1 vs S2	80.04	15.70 to 144.4	P=0.0063, **
	Preference; Ordinary one-way ANOVA; Dunnett's. comparison test	+/+ vs +/-	-15.89	-64.84 to 33.06	P=0.6792, ns
		+/+ vs -/-	15.19	-39.46 to 69.85	P=0.7503, ns
Fig 1C 3C_sociability; Male	Interaction time; Two-way ANOVA; Tukey's HSD multiple comparison test	+/+: S1 vs O	225.5	189.9 to 261.1	P<0.0001, ****
		M120I: S1 vs O	81.53	45.93 to 117.1	P<0.0001, ****
		S1: +/+ vs M120I	121.5	85.93 to 157.1	P<0.0001, ****
	Unpaired t test	+/+ vs M120I	Two-tailed	t=8.340, df=28	P<0.0001, ****
Fig 1C 3C_sociability; female	Preference; Two-way ANOVA; Tukey's HSD multiple comparison test	+/+: S1 vs O	189.7	149.3 to 230.1	P<0.0001, ****
		M120I: S1 vs O	177.9	136.0 to 219.8	P<0.0001, ****
	Unpaired t test	+/+ vs M120I	Two-tailed	t=0.4220, df=25	P=0.677, ns
Fig. 1C 3C_ novelty preference; Male	Interaction time; Two-way ANOVA; Tukey's HSD multiple comparison test	+/+: S1 vs S2	143.2	98.24 to 188.2	P<0.0001, ****
		M120I: S1 vs S2	22.53	-22.42 to 67.49	P=0.55, ns
		S2: +/+ vs M120I	103.8	58.84 to 148.8	P<0.0001, ****
	Unpaired t test	+/+ vs M120I	Two-tailed	t=7.978, df=28	P<0.0001, ****
Fig. 1C 3C_novelty preference; Female	Preference; Two-way ANOVA; Tukey's HSD multiple comparison test	+/+: S1 vs S2	121.9	83.74 to 160.0	P<0.0001, ****
		M120I: S1 vs S2	119.9	80.37 to 159.5	P<0.0001, ****

	Unpaired t test	+/+ vs M120I	Two-tailed	t=0.08710, df=25	P=0.9313, ns
Fig. 1D. RSI; Male	Ordinary one-way ANOVA; Dunnett's. comparison test	+/+ vs +/-	40.92	1.489 to 80.36	P=0.0411, *
		+/+ vs -/-	65.85	26.41 to 105.3	P=0.0009, ***
	Unpaired t test	+/+ vs M120I	Two-tailed	t=5.645, df=28	P<0.0001, ****
Fig. 1D. RSI; Female	Ordinary one-way ANOVA; Dunnett's. comparison test	+/+ vs +/-	18.24	-11.02 to 47.51	P=0.2717, ns
		+/+ vs -/-	-15.65	-48.32 to 17.02	P=0.4469, ns
	Unpaired t test	+/+ vs M120I	Two-tailed	t=0.4106, df=25	P=0.6849, ns
Fig. 3B Male	Unpaired t test	ACAd,Ctrl vs hM3Dq	Two-tailed	t=0.04856, df=7	P=0.96, ns
		PL, Ctrl vs hM3Dq	Two-tailed	t=1.153, df=7	P=0.2867, ns
		ILA, Ctrl vs hM3Dq	Two-tailed	t=4.063, df=8	P=0.0036, **
Fig. 3C. Male	Paired t test	C21- vs C21+	Two-tailed	t=0.8659, df=8	P=0.4118, ns
	Paired t test	C21- vs C21+	Two-tailed	t=8.879, df=11	P<0.0001, ****
	Unpaired t test	Ctrl vs hM3Dq	Two-tailed	t=6.984, df=19	P<0.0001, ****
	Unpaired t test	Ctrl vs hM3Dq	Two-tailed	t=7.521, df=19	P<0.0001, ****
Fig. 3D Male	Paired t test	C21- vs C21+	Two-tailed	t=2.806, df=9	P=0.0205, *
	Paired t test	C21- vs C21+	Two-tailed	t=1.180, df=10	P=0.2652, ns
	Unpaired t test	Ctrl vs hM3Dq	Two-tailed	t=0.2972, df=19	P=0.7695, ns
	Unpaired t test	Ctrl vs hM3Dq	Two-tailed	t=0.2031, df=19	P=0.8412, ns
Fig. 3E. Female	Paired t test	C21- vs C21+	Two-tailed	t=2.751, df=10	P=0.0205, *
	Paired t test	C21- vs C21+	Two-tailed	t=11.68, df=14	P<0.0001, ****
	Unpaired t test	Ctrl vs hM4Di	Two-tailed	t=7.617, df=24	P<0.0001, ****
	Unpaired t test	Ctrl vs hM4Di	Two-tailed	t=4.813, df=24	P<0.0001, ****
Fig. 3F Female	Paired t test	C21- vs C21+	Two-tailed	t=2.310, df=11	P=0.0413, *
	Paired t test	C21- vs C21+	Two-tailed	t=11.96, df=10	P<0.0001, ****
	Unpaired t test	Ctrl vs hM4Di	Two-tailed	t=7.779, df=21	P<0.0001, ****
	Unpaired t test	Ctrl vs hM4Di	Two-tailed	t=9.233, df=21	P<0.0001, ****
Fig. 3G. Male	Unpaired t test	LSr	Two-tailed	t=1.370, df=8	P=0.2080, ns
		MS	Two-tailed	t=1.310, df=8	P=0.2266, ns
		BSTam	Two-tailed	t=2.386, df=8	P=0.0442, *
		DGd	Two-tailed	t=3.513, df=8	P=0.0079, **
		LA	Two-tailed	t=1.495, df=8	P=0.1734, ns
		BLAa	Two-tailed	t=2.933, df=8	P=0.0189,*
		LH	Two-tailed	t=1.335, df=8	P=0.2185, ns
		VTA	Two-tailed	t=3.871, df=8	P=0.0047, **
Fig. 4G Male_SHANK2	Unpaired t test	WT vs M120I	Two-tailed	t=3.397, df=9	P=0.0079, **
Fig. 4G Female_SHANK2		WT vs M120I	Two-tailed	t=0.2362, df=10	P=0.8181, ns
Fig. 4G Male_SYNPO		WT vs M120I	Two-tailed	t=2.236, df=11	P=0.0470, *
Fig. 4G Female_SYNPO		WT vs M120I	Two-tailed	t=1.067, df=12	P=0.3069, ns
Fig. 4G Male_PSD-95		WT vs M120I	Two-tailed	t=6.040, df=11	P<0.0001, ****

Fig. 4G Female_PSD-95		WT vs M120I	Two-tailed	t=0.2810, df=12	P=0.7835, ns
Fig. 4H Male_RRAGC		WT vs M120I	Two-tailed	t=0.3015, df=9	P=0.7699, ns
Fig. 4H Female_RRAGC		WT vs M120I	Two-tailed	t=2.649, df=10	P=0.0244, *
Fig. 4H Male_TIPRL		WT vs M120I	Two-tailed	t=1.892, df=12	P=0.0829, ns
Fig. 4H Female_TIPRL		WT vs M120I	Two-tailed	t=2.287, df=11	P=0.043, *
Fig. 4I Female_p-mTOR		WT vs M120I	Two-tailed	t=3.083, df=10	P=0.0116, *
Fig. 5B Male	Unpaired t test	P-mTOR/mTOR water	Two-tailed	t=3.965, df=6	P=0.0074, **
		P-mTOR/mTOR BCAA	Two-tailed	t=2.881, df=6	P=0.028, *
		P-S6K/S6K water	Two-tailed	t=2.741, df=6	P=0.0337, *
		P-S6K/S6K BCAA	Two-tailed	t=2.724, df=6	P=0.0345, *
		4EBP/HSP90 water	Two-tailed	t=0.3334, df=6	P=0.7502, ns
		4EBP/HSP90 BCAA	Two-tailed	t=0.1705, df=6	P=0.8702, ns
Fig. 5C Male	Two-way ANOVA; Tukey's HSD multiple comparison test	WT: BCAA-/BCAA+	0.6868	-0.9502 to 2.324	P=0.6951, ns
		BCAA-: WT vs M120I	5.16	3.464 to 6.856	P<0.0001, ****
		M120I: BCAA-/BCAA+	-6.569	-8.423 to -4.714	P<0.0001, ****
		BCAA + : WT vs M120I	-2.096	-3.897 to -0.2947	P=0.0155, *
	Two-way ANOVA; Tukey's HSD multiple comparison test	WT: BCAA-/BCAA+	-0.001712	-0.02572 to 0.02230	P=0.998, ns
		BCAA-: WT vs M120I	0.08229	0.05742 to 0.1072	P<0.0001, ****
		M120I: BCAA-/BCAA+	-0.06098	-0.08818 to -0.03378	P<0.0001, ****
		BCAA + : WT vs M120I	0.02303	-0.003391 to 0.04944	P=0.1108, ns
	Two-way ANOVA; Tukey's HSD multiple comparison test	WT: BCAA-/BCAA+	-0.06752	-0.1377 to 0.002625	P=0.0638, ns
		BCAA-: WT vs M120I	0.1339	0.06120 to 0.2065	P<0.0001, ****
		M120I: BCAA-/BCAA+	-0.1543	-0.2337 to -0.07479	P<0.0001, ****
		BCAA + : WT vs M120I	0.04712	-0.03005 to 0.1243	P=0.3883, ns
Fig. 5D Male	Two-way ANOVA; Tukey's HSD multiple comparison test	WT: BCAA-/BCAA+	-19.37	-41.37 to 2.618	P=0.1027, ns
		BCAA-: WT vs M120I	80.43	59.57 to 101.3	P<0.0001, ****
		M120I: BCAA-/BCAA+	-94.71	-116.0 to -73.47	P<0.0001, ****
		BCAA + : WT vs M120I	5.093	-17.26 to 27.45	P=0.9304, ns
Fig. 5E Male	Unpaired t test	WT vs M120I	Two-tailed	t=5.124, df=6	P=0.0022, **
		WT vs M120I	Two-tailed	t=0.05818, df=6	P=0.9555, ns
Fig. 5F Male	Paired t test	BCAA- vs BCAA+	Two-tailed	t=4.121, df=7	P=0.0045, **

Fig. 6B 150 ppm 3C_sociability, Male	Interaction times; Two-way ANOVA; Tukey's HSD multiple comparison test	S1 vs O	194.3	159.7 to 228.9	P<0.0001, ****
		S1 vs O	175.2	144.8 to 205.6	P<0.0001, ****
	Unpaired t test	WT vs M1201	Two-tailed	t=0.8415, df=21	P=0.4095, ns
Fig. 6B 150 ppm 3C_novelty preference, Male	Interaction time; Two-way ANOVA; Tukey's HSD multiple comparison test	S1 vs S2	129	77.01 to 181.0	P<0.0001, ****
		S1 vs S2	89.08	43.48 to 134.7	P<0.0001, ****
	Unpaired t test	WT vs M1201	Two-tailed	t=1.381, df=21	P=0.1819, ns
Fig. 6B 150 ppm RSI, Male	Unpaired t test	WT vs M1201	Two-tailed	t=2.380, df=21	P=0.0269, *
Fig. 6B 150 ppm, 3C_sociability, Female	Two-way ANOVA; Tukey's HSD multiple comparison test	S1 vs O	188.5	150.7 to 226.3	P<0.0001, ****
		S1 vs O	187.1	149.3 to 224.9	P<0.0001, ****
	Unpaired t test	WT vs M1201	Two-tailed	t=0.07192, df=18	P=0.9435, ns
Fig. 6B 150 ppm, 3C_novelty preference, Female	Two-way ANOVA; Tukey's HSD multiple comparison test	S1 vs S2	102.1	60.76 to 143.4	P<0.0001, ****
		S1 vs S2	86.7	45.36 to 128.0	P<0.0001, ****
	Unpaired t test	WT vs M1201	Two-tailed	t=0.8270, df=18	P=0.4191, ns
Fig. 6B 150 ppm, RSI, Female	Unpaired t test	WT vs M1201	Two-tailed	t=0.5314, df=18	P=0.6016, ns
Fig. 6C 30 ppm, 3C_sociability, male	Two-way ANOVA; Tukey's HSD multiple comparison test	S1 vs O	194.3	150.6 to 237.9	P<0.0001, ****
		S1 vs O	61.85	21.71 to 102.0	P=0.0009, ***
	Unpaired t test	WT vs M1201	Two-tailed	t=6.562, df=22	P<0.0001, ****
Fig. 6C 30 ppm, 3C_novelty preference, male	Two-way ANOVA; Tukey's HSD multiple comparison test	S1 vs S2	106	57.41 to 154.6	P<0.0001, ****
		S1 vs S2	4.462	-40.24 to 49.16	P=0.9933, ns
	Unpaired t test	WT vs M1201	Two-tailed	t=6.913, df=22	P<0.0001, ****
Fig. 6C 30 ppm, RSI, male	Unpaired t test	WT vs M1201	Two-tailed	t=4.901, df=22	P<0.0001, ****
Fig. 6C 30 ppm, 3C_sociability, Female	Two-way ANOVA; Tukey's HSD multiple comparison test	S1 vs O	177.1	134.5 to 219.7	P<0.0001, ****
		S1 vs O	207	164.4 to 249.6	P<0.0001, ****
	Unpaired t test	WT vs M1201	Two-tailed	t=1.331, df=20	P=0.1981, ns
Fig. 6C 30 ppm 3C_novelty preference, Female	Two-way ANOVA; Tukey's HSD multiple comparison test	S1 vs S2	98.09	54.00 to 142.2	P<0.0001, ****
		S1 vs S2	94.18	50.09 to 138.3	P<0.0001, ****
	Unpaired t test	WT vs M1201	Two-tailed	t=0.1911, df=20	P=0.8504, ns
Fig. 6C 30 ppm, RSI, Female	Unpaired t test	WT vs M1201	Two-tailed	t=0.4271, df=20	P=0.6738, ns